Tampere University

Mehmet Ferlibas

LOAD WEIGHT ESTIMATION ON EXCAVATORS

Faculty of Engineering and Natural Sciences (ENS)
Master of Science thesis
Examiners and topic approved on 23 September 2020

Abstract

Mehmet Ferlibas: Load Weight Estimation on Excavators
Master of Science thesis
Tampere University
Degree Programme in Automation Engineering, MSc (Tech)
October 2020

Excavators are widely used in earth moving operations. There is a need for payload monitoring systems on these hydraulically operating machines in order to prevent the possible problems while transferring the material, increase the efficiency, and obtain the product information automatically.

This research proposes a method for estimating the load weight in the excavator's bucket. The problem was separated to two parts as static estimation and dynamic estimation of the load weight. The collected data is processed offline and a parameter estimation process was performed in both of the static estimation and dynamic estimation by using least squares estimation of parameters to predict the no load torque values. There was a need to estimate the angular velocities and angular accelerations from the angular position measurements in order to utilize the method in dynamic estimation. The angular velocity measurements are used as reference to observe the accuracy of the angular velocity estimations. The friction is neglected in modeling throughout the work. However, the effect of the static friction is obviously present in the collected data.

The method was tested with two different load weights in each of the static estimation and the dynamic estimation. The results obtained showed that the static friction plays an important role in static estimation. However, the developed method provides accurate enough results that the error in dynamic load weight estimation is less than 2% for high enough velocities. Finally, further improvements are suggested in the end of this work.

Keywords: Payload estimation, excavator, hydraulic machine, hydraulic manipulator, robotics, parameter estimation,least squares estimation

Preface

This thesis was a part of the MIDAS Project at Tampere University. I would like to thank my supervisors Assoc. Prof. Reza Ghbcheloo and Dr. Pavel Davidson for giving me the opportunity of working with them and their help throughout my thesis process. Also, I thank the engineers at Novatron Oy for their guidance as they were always communicative when I needed to ask any question regarding the excavator data that is provided by Novatron Oy and used in this work. I can't explain in words how thankful I am to my family and my girlfriend for their support during my M.Sc. studies and this thesis work.

Tampere, 19 October 2020

Contents

List of Figures

List of Tables

List of Symbols

α_2	Constant angle between a_2 and r_2
α_3	Constant angle between a_3 and r_3
α_4	Constant angle between a_4 and r_4
β_1	Offset angle used to obtain boom joint variable
β_2	Offset angle used to obtain boom joint variable
β_3	Offset angle used to obtain stick joint variable
β_4	Offset angle used to obtain stick joint variable
$\hat{M}$	Load mass in the bucket
τ_2	Boom joint torque
τ_3	Stick joint torque
τ_4	Bucket joint torque
θ_2	Boom angular position
θ_3	Stick angular position
θ_4	Bucket angular position
a_2	Linear displacement between the boom joint and the stick joint
a_3	Linear displacement between the stick joint and the bucket joint
a_4	Linear displacement between the bucket joint and the bucket tip
I_{bo}	Inertia of the boom link
I_{bu}	Inertia of the bucket link
I_{st}	Inertia of the stick link
J_{bo}	Boom jacobian
J_{bu}	Bucket jacobian
J_{st}	Stick jacobian
L_{11}	Distance between boom joint and one end of the hydraulic actuator

L_{12} Distance between boom joint and the other end of the hydraulic actuator

L_{21} Distance between stick joint and one end of the hydraulic actuator

L_{22} Distance between stick joint and the other end of the hydraulic actuator

M_{bo} Mass of the boom link

M_{bu} Mass of the bucket link

M_{st} Mass of the stick link

q_2 Boom joint variable

q_3 Stick joint variable

q_4 Bucket joint variable

r_2 Distance vector from origin of the attached coordinate frame to the boom center of gravity

r_3 Distance vector from origin of the attached coordinate frame to the stick center of gravity

r_4 Distance vector from origin of the attached coordinate frame to the bucket center of gravity

z_2 Length of the boom hydraulic actuator

z_3 Length of the stick hydraulic actuator

z_4 Length of the bucket hydraulic actuator

1 INTRODUCTION

Excavators are essential in earth moving operations. These heavy construction equipment are considered as hydraulic machines since the fluid power is used in their structure to perform work. These hydraulically actuated manipulators are not only used in construction sites, but also they are widely used in forestry, agriculture and mining. Considering a construction site, excavators are the first candidates to dig and move the rocks and soil from one place to another place, with the help of trucks for removal purposes.

There is a payload capacity for each truck that should not be exceeded. Otherwise, serious problems such as tire blowouts, suspension system failures or difficulty in controlling the steering wheel may occur. Moreover, the truck scales are not always available to measure the gross weight of the trucks in the work sites. In order to prevent these kind of problems and to improve the productivity and the efficiency, payload monitoring systems are needed. It is possible to estimate the load weight for each digging cycle of an excavator, meaning that the overall payload delivered to trucks can be calculated cumulatively and automatically.

There are existing load weight estimation algorithms for heavy duty hydraulic machines. For example, there are techniques proposed for wheel loaders [1, 10], mini excavators [32], and excavators [6, 26, 35, 36].

In order to develop such weighing algorithms, the structural similarity of these hydraulically operating machines to the serial robot manipulators has been benefited. The links of an excavator, namely the boom, the stick, and the bucket operate with the help of the hydraulic actuators. Therefore, the change in the joint angle is described as a function of linear displacement in the hydraulic cylinders [9]. In the light of this information, the excavators can be considered as serial robot manipulators [32, 33, 34, 36]. Hence, the existing algorithms of the field of robotics can be used in order to study the excavator dynamics.

Numerous research have been conducted in order to identify the parameters of the robot manipulators such as the link lengths, link masses, moments of inertia, and centers of gravity [5, 14, 16]. Also, there are studies in which the parameter estimation for excavators has been discussed [32, 33, 34, 36, 35, 37, 38] as these parameters are needed in developing weighing algorithms. Thus, parameter estimation has been performed first, before proceeding with the load weight estimation [4, 7, 34, 36].

1.1 The focus of this thesis

This study focuses on solving the load weight estimation problem using a Komatsu PC138US-8 hydraulic excavator that is provided by Novatron Oy. The problem is divided into two parts as static estimation of the load weight and dynamic estimation of the load weight using angular position measurements of the links and pressure readings from the hydraulic cylinders.

In the static load weight estimation part, a proposed approach that is tested on mini excavators [34] has been utilized. The approach presents three methods based on the difference between the torque values with and without the load for the same stationary pose of the excavator links. The same idea of using the torque differences is extended to the dynamic estimation with an assumption that the bucket's center of gravity remains unchanged with different load masses in the bucket.

In both of the static and dynamic estimations of the load weight, the torque equations obtained using Newton-Lagrange method [33] has been used.

1.2 The structure of this thesis

The machine instrumentation and the sensors used are explained in Chapter 2. The system dynamics is presented in Chapter 3. The static estimation of the load weight and the dynamic estimation of the load weight and the results obtained are discussed in detail in the Chapters 4 and 5, respectively. The conclusions are given in the Chapter 6 and future work is stated in Chapter 7.

2 MACHINE INSTRUMENTATION

The excavator, whose CAD model is illustrated in the Figure 2.1, is considered as a three-revolute joint hydraulic manipulator in the vertical plane with the boom link, the stick link and the bucket link. There are four IMU sensors located in the cabin frame, boom linkage, stick linkage, and bucket linkage of the excavator in order to measure the angular positions and the angular velocities of each link. In the collected data, the boom angle is recorded with respect to cabin frame, the stick angle is recorded with respect to the boom and the bucket angle is recorded with respect to the stick. Moreover, there are two pressure sensors that are used in each cylinder to measure the fluid pressures inside the cylinder chambers. That is, there are six pressure sensors installed on the machine. All of the sensors operate at a frequency of 200 Hz.

The Figure 2.1 shows how the joint angles θ_2, θ_3 and θ_4 are measured for the boom, the stick, and the bucket, respectively. Note that index 1 is reserved for the cabin frame which is excluded from the scope of this research. The constant angles β_1, β_2, β_3, and β_4 are used to obtain the joint variables q_2 and q_3. The constant lengths from the joints to the actuator ends are labeled as L_{11}, L_{12}, L_{21}, and L_{22} that are used to calculate the actuator lengths z_2 and z_3. These lengths from the joints to the actuator ends and constant angle values are obtained from the CAD model. The Section 3.3 describes how and why the actuator lengths and the joint variables are calculated. The distance from the boom joint to the stick joint is a_2. Similarly, a_3 represents the distance from the stick joint to the bucket joint and a_4 stands for the distance between the bucket joint and the bucket tip. These linear displacements between the joints are obtained from the data-sheet of the excavator [15].

The Figure 2.2 is the simplest schematic of the excavator in which the boom, the stick and the bucket is shown. Polar coordinates of center of gravities of each link are represented with (r_i, cg_i). τ_2 is the torque exerted in the boom joint, where τ_3 and τ_4 are the torques exerted in the stick and the bucket joints, respectively. The angular position of the stick linkage with respect to the horizontal plane is θ_{23} and $\theta_{23} = \theta_2 + \theta_3$. In the same way, the angular position of the bucket linkage with respect to the horizontal plane is θ_{234} and $\theta_{234} = \theta_{23} + \theta_4 + c$ where the value c is a constant offset angle that is used to obtain the position of the bucket tip with respect to the horizontal plane. More detailed information about calculation of the position of the bucket tip with respect to horizontal plane is provided in the Chapter 3.

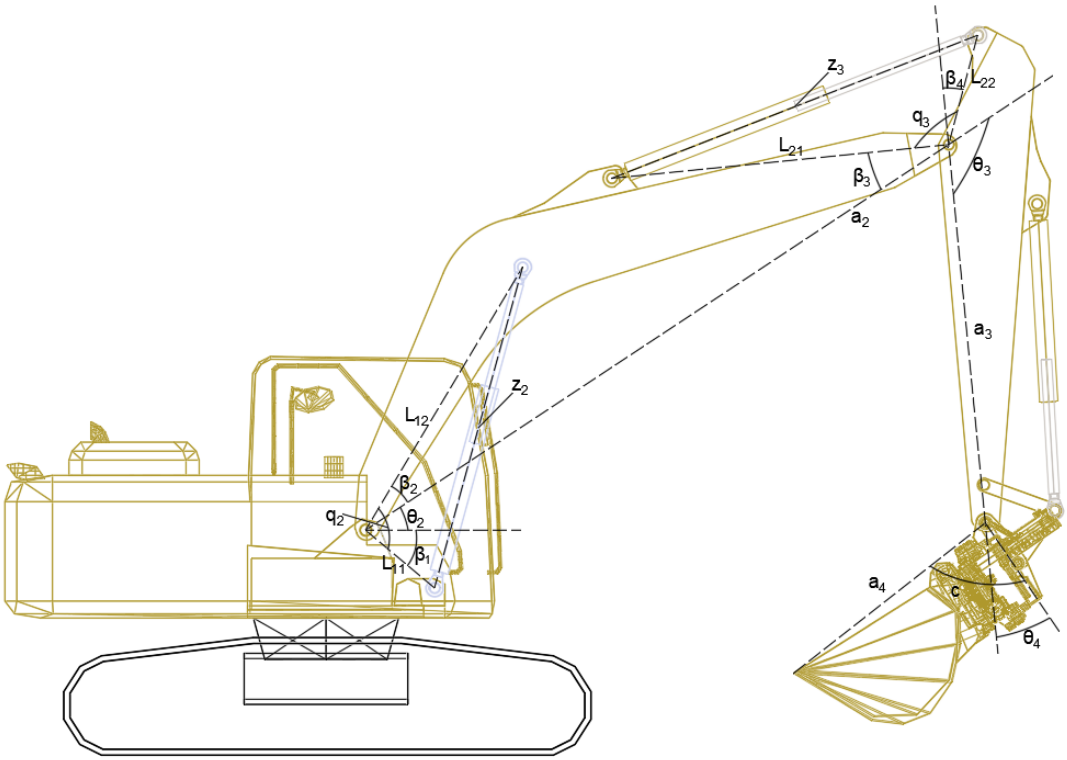

Figure 2.1 *Excavator CAD model*

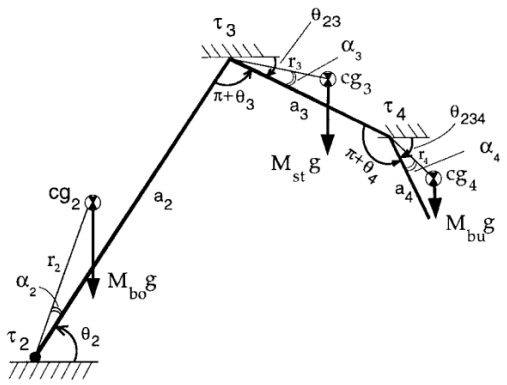

Figure 2.2 *Excavator schematic diagram [34]*

3 SYSTEM DYNAMICS

The excavator can be considered as a planar manipulator that has 3 revolute joints by excluding the cabin swing from the study [34] and assuming that the tiltrotator is only a series of offsets.

The dynamic model of a manipulator described above can be expressed by the following differential equation [4, 21, 26]:

$$\tau = D(\Theta)\ddot{\Theta} + C(\Theta, \dot{\Theta})\dot{\Theta} + G(\Theta) \tag{3.1}$$

Where,

- τ is the joint torque vector,
- Θ is the vector of joint angles,
- $D(\Theta)$ is the inertia matrix,
- $C(\Theta, \dot{\Theta})\dot{\Theta}$ is the vector of Coriolis and centrifugal terms,
- G(Θ) is the gravity torque vector.

One strong property of the equation (3.1) is that it can be converted to following form in the equation (3.2), which is linear in the dynamic parameters [11, 30, 34]:

$$\tau = Y(\Theta, \dot{\Theta}, \ddot{\Theta})\pi \tag{3.2}$$

Where $Y(\Theta, \dot{\Theta}, \ddot{\Theta})$ is the matrix of functions of joint positions, velocities and accelerations and π is the vector of dynamic parameters which are assumed to be constant values.

Assuming that the summation of the kinetic energy and the potential energy of the system is constant, meaning that the friction is non-existent; therefore, the system is conservative and the cabin is stationary [33, 34], the following torque equations (3.3) were obtained using Euler-Lagrange method:

$$\begin{aligned}
\tau_4 &= (I_{bu} + M_{bu}r_4^2)\ddot{\theta}_{234} + M_{bu}a_2r_4[\ddot{\theta}_2 cos(\theta_{34} + \alpha_4) + \dot{\theta}_2^2 sin(\theta_{34} + \alpha_4)] \\
&\quad + M_{bu}a_3r_4[\ddot{\theta}_{23} cos(\theta_4 + \alpha_4) + \dot{\theta}_{23}^2 sin(\theta_4 + \alpha_4)] + M_{bu}gr_4 cos(\theta_{234} + \alpha_4) \\
\tau_3 &= \tau_4 + (I_{st} + M_{st}r_3^2 + M_{bu}a_2^3)\ddot{\theta}_{23} + M_{bu}a_2a_3(\ddot{\theta}_2 cos(\theta_3) + \dot{\theta}_2^2 sin(\theta_3)) \\
&\quad + M_{bu}a_3r_4[\ddot{\theta}_{234}(\theta_4 + \alpha_4) - \dot{\theta}_{234}^2 sin(\theta_4 + \alpha_4)] \\
&\quad + M_{st}a_2r_3[\ddot{\theta}_2 cos(\theta_3 + \alpha_3) + \dot{\theta}_2^2 sin(\theta_3 + \alpha_3)] \\
&\quad + M_{bu}ga_3 cos(\theta_{23}) + M_{st}gr_3 cos(\theta_{23} + \alpha_3)
\end{aligned}$$

$$\begin{aligned}\tau_2 = \tau_3 &+ [I_{bo} + M_{bo}r_2^2 + (M_{st} + M_{bu})a_2^2]\ddot{\theta}_2 \\ &+ M_{st}a_2r_3[\ddot{\theta}_{23}cos(\theta_3 + \alpha_3) - \dot{\theta}_{23}^2 sin(\theta_3 + \alpha_3)] \\ &+ M_{bu}a_2a_3(\ddot{\theta}_{23}cos(\theta_3) - \dot{\theta}_{23}^2 sin(\theta_3) \\ &+ M_{bu}a_2r_4[\ddot{\theta}_{234}cos(\theta_{34} + \alpha_4) - \dot{\theta}_{234}^2 sin(\theta_{34} + \alpha_4)] \\ &+ (M_{bu} + M_{st})ga_2cos(\theta_2) + M_{bo}gr_2cos(\theta_2 + \alpha_2) \end{aligned} \tag{3.3}$$

Where I_{bo}, I_{st}, I_{bu} stand for the moments of inertia of the boom link, the stick link and the bucket link, respectively. Masses of the boom link, the stick link and the bucket link are represented with the notations M_{bo}, M_{st}, M_{bu}, separately. It should be noted that the angular position of the bucket tip has to be acquired as stated in the Chapter 2 since the position of the bucket tip is taken into account in the equation (3.3). The following Section 3.1 describes how to obtain the angular position of the bucket tip with respect to the ground.

3.1 Calculation of bucket tip's angular position

In order to use the torque equations given in the equation (3.3), the angular position of the bucket tip with respect to the stick link has to be calculated. As can be seen in the Figure 2.1, angular position of the bucket tip is not recorded directly since the IMU sensor of the bucket is located at the four-bar linkage of the excavator. An offset angle, c that is also shown in the Figure 2.1, has to be added to the recorded angular position of the bucket to acquire the angular position of the bucket tip with respect to the stick link. The lengths describing the offset angle are illustrated by the following Figure 3.1. Once the position of the bucket tip with respect to the stick is obtained, the position of the bucket tip with respect to the horizontal plane can be calculated by simply adding this quantity to the boom angular position and the stick angular position.

Figure 3.1 *Lengths needed in mapping of angular position of the bucket tip with respect to the ground*

The distance to the bucket tip along the attached coordinate frame x-axis is measured as -332.5 mm and the distance to the bucket tip along the attached coordinate frame y-axis is measured as -1252.2 mm. Therefore, the offset angle c can be calculated as given in the equation (3.4) below:

$$c = -\frac{\pi}{2} - tan^{-1}\left(\frac{-332.5}{-1252.2}\right) = -104.87° \tag{3.4}$$

3.2 Force calculations using pressure data

In order to obtain the torque values given in the equation (3.3), the pressure readings that are collected by the pressure sensors can be used. The following well-known equation is used to obtain the net force exerted in the hydraulic cylinders [3]:

$$F = P_1 A_1 - P_2 A_2 \tag{3.5}$$

Where P_1 and P_2 are the pressures in the chamber A and chamber B of the hydraulic cylinder and A_1 and A_2 are the cross-sectional areas of the chamber A and chamber B of the hydraulic cylinder, respectively.

3.3 Mapping of actuator forces to joint torques

The forces generated in the hydraulic actuators are mapped to the joint torques using the equation (3.6) below, where J is the cylinder jacobian.

$$\tau = J^T(\theta)F \tag{3.6}$$

Note that $J^T(\theta) = J(\theta)$, since the cylinder jacobians are scalar quantities for each link. In order to obtain these cylinder Jacobians, a relation between the actuator length and the joint angle for each link has to be constructed first. In order to calculate the actuator lengths, the joint angles are mapped to joint variables (q). Then, actuator lengths are calculated as functions of these joint variables using the cosine law. Finally, the cylinder jacobians are calculated by taking the derivative of the actuator lengths with respect to the joint angles.

3.3.1 Boom cylinder jacobian

As discussed earlier in the Chapter 2, the joint angle θ_2 is measured with respect to the cabin frame as can be seen the Figure 3.2. β_1 and β_2 are constant offset angles that are used to obtain q_2, which is the joint variable that is used to relate the actuator length, z_2, with the joint angle θ_2. Similarly, L_{11} and L_{12} are constant lengths from the boom joint to both ends of the hydraulic actuator. The equations (3.7), (3.8), and (3.9) show how the boom cylinder Jacobian, J_{bo}, is obtained:

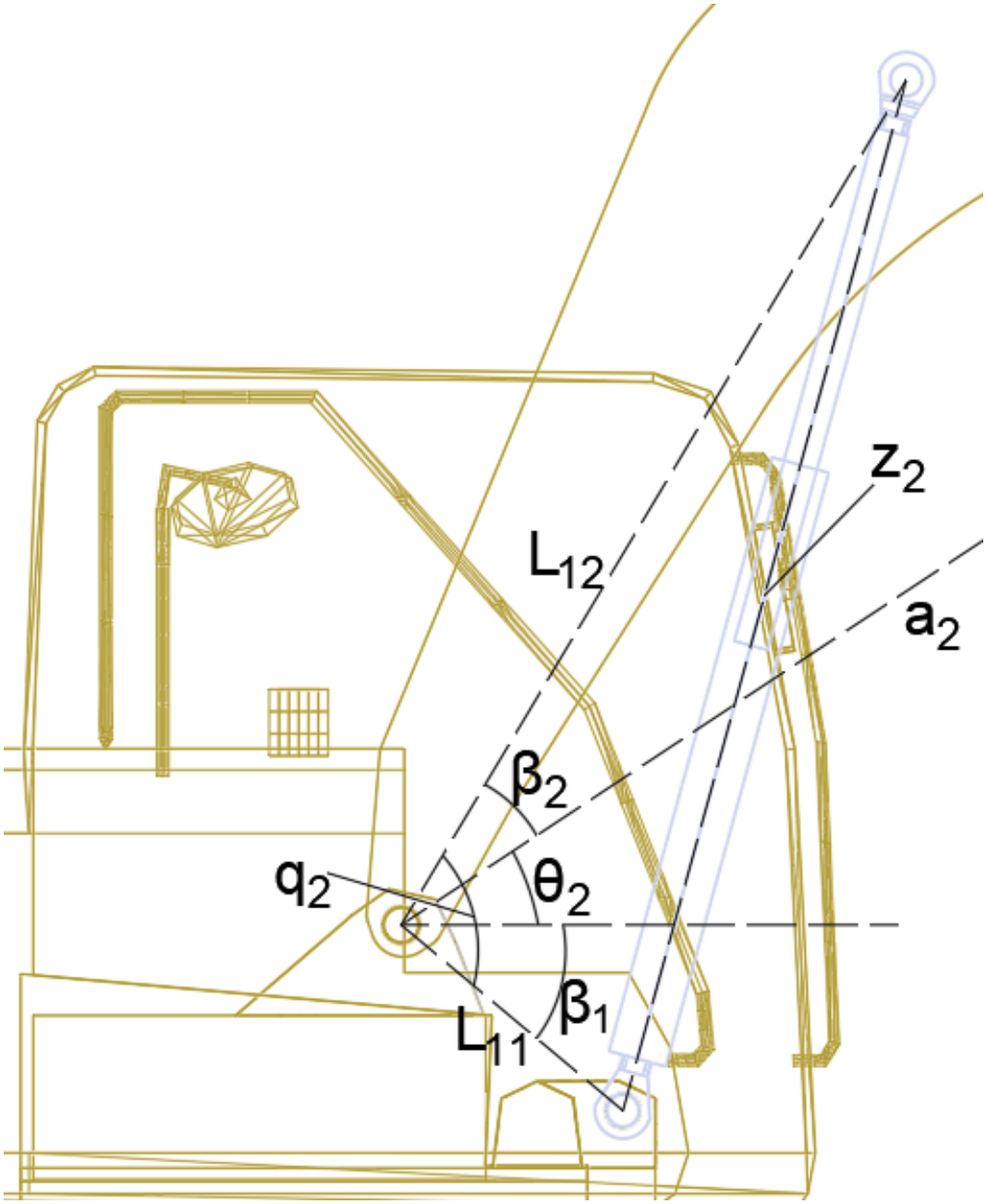

Figure 3.2 *Boom joint angle and joint variable*

$$q_2 = \beta_1 + \beta_2 + \theta_2 \tag{3.7}$$

$$z_2 = \sqrt{L_{11}^2 + L_{12}^2 - 2L_{11}L_{12}cos(q_2)} \tag{3.8}$$

$$J_{bo} = \frac{dz_2}{d\theta_2} = \frac{L_{11}L_{12}sin(q_2)}{z_2} \tag{3.9}$$

3.3.2 Stick cylinder jacobian

The stick angular position measurements are taken with respect to the distance vector a_2 between the boom joint and the stick joint, and represented by θ_3, which can be seen in the Figure 3.3. The joint variable is labeled as q_3 and the actuator length is z_3. Similar to the case for the boom jacobian that is introduced in the Section 3.3.1, β_3 and β_4 are constant offset angles and L_{21} and L_{22} are constant distances from the stick joint to the both ends of the hydraulic actuator. Stick jacobian, J_{st}, is obtained by following the equations (3.10), (3.11), and (3.12).

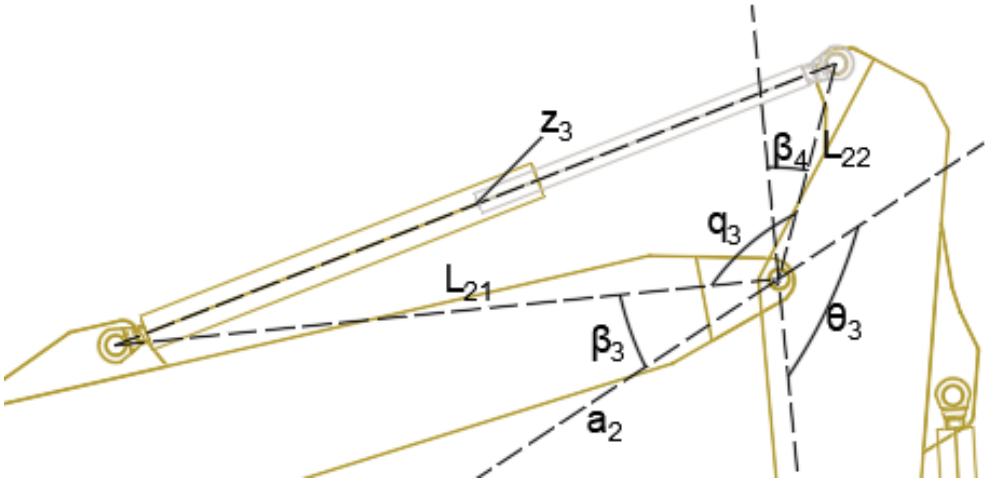

Figure 3.3 *Stick joint angle and joint variable*

$$q_3 = \beta_4 - \beta_3 - \theta_3 \tag{3.10}$$

$$z_3 = \sqrt{L_{21}^2 + L_{22}^2 - 2L_{21}L_{22}cos(q_3)} \tag{3.11}$$

$$J_{st} = \frac{dz_3}{d\theta_3} = -\frac{L_{21}L_{22}sin(q_3)}{z_3} \tag{3.12}$$

It should be noted that the stick angular position is negative as the rotation is clockwise. Therefore, increase in the stick angular position means that the actuator length Z_3 decreases. That is why a minus sign is introduced in the equation (3.12) different than calculation of the boom jacobian.

3.3.3 Bucket cylinder jacobian

Since the IMU sensor is located on the dog bone, converting the joint angle to the joint variable is harder compared to the boom and the stick. The bucket angular

position measurements are taken with respect to the stick linkage and represented by θ_4, which can be seen in the Figure 3.4.

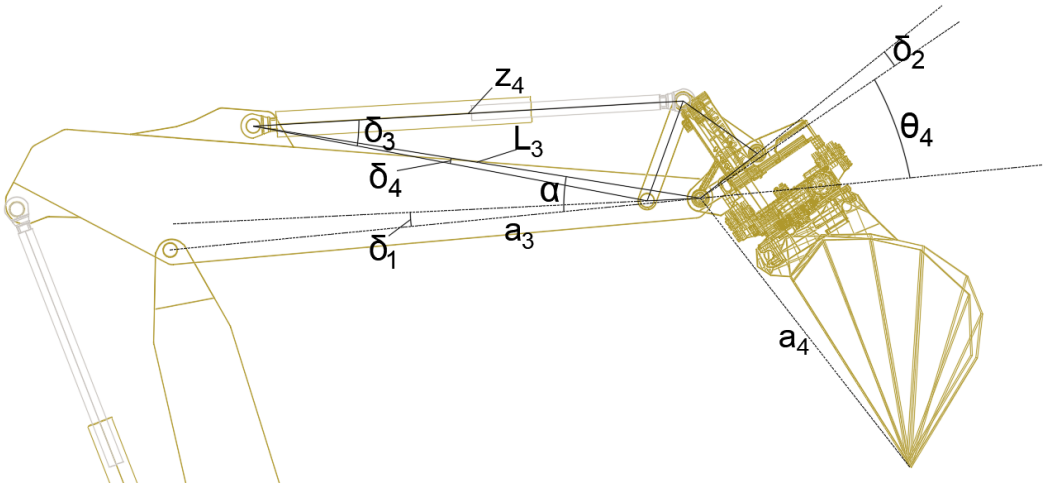

Figure 3.4 *Bucket joint angle and offset angles*

The constant angles δ_1, δ_2, δ_3, δ_4, and α are used to obtain the joint variable q_4 that is shown in the Figure 3.5. The lengths of the links forming the four bar linkage are represented by c_1, c_2, c_3, and c_4. The imaginary diagonal lines are illustrated as x and y.

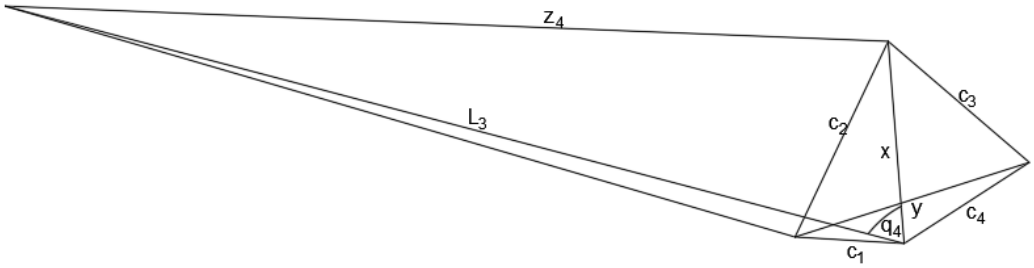

Figure 3.5 *Four bar linkage schematics*

Define the following angles to construct the relation between the joint variable q_4 and the joint angle θ_4:

- q_4 is the angle between L_3 and x.
- β_{51} is the angle between c_1 and c_4,
- β_{52} is the angle between c_1 and c_2,
- β_{53} is the angle between c_2 and c_3,
- σ_1 is the angle between c_2 and y,

- σ_2 is the angle between c_1 and y,
- σ_3 is the angle between c_1 and x.

The equations (3.13) to (3.21) describe how the joint variable q_4 is obtained using the parameters c_1, c_2, c_3, and c_4 together with the bucket angular measurement θ_4, using the variables defined above.

$$\beta_{51} = \pi - \theta_4 - \delta_1 - \delta_2 \tag{3.13}$$

$$y = \sqrt{c_1^2 + c_4^2 - 2c_1c_4cos(\beta_{51})} \tag{3.14}$$

$$\beta_{53} = cos^{-1}\left(\frac{y^2 - c_2^2 - c_3^2}{-2c_2c_3}\right) \tag{3.15}$$

$$\sigma_1 = sin^{-1}\left(\frac{c_3sin(\beta_{53})}{y}\right) \tag{3.16}$$

$$\sigma_2 = sin^{-1}\left(\frac{c_4sin(\beta_{51})}{y}\right) \tag{3.17}$$

$$\beta_{52} = \sigma_1 + \sigma_2 \tag{3.18}$$

$$x = \sqrt{c_1^2 + c_2^2 - 2c_1c_2cos(\beta_{52})} \tag{3.19}$$

$$\sigma_3 = cos^{-1}\left(\frac{c_2^2 - c_1^2 - x^2}{-2c_1x}\right) \tag{3.20}$$

$$q_4 = \sigma_3 - \alpha + \delta_1 \tag{3.21}$$

After obtaining the joint variable q_4, the following equations (3.22) and (3.23) are used in order to calculate the actuator length z_4 and the bucket jacobian J_{bu}, respectively:

$$z_4 = \sqrt{L_3^2 + x^2 - 2L_3xcos(q_4)} \tag{3.22}$$

$$J_{bu} = \frac{dz_4}{d\theta_4} = -\frac{L_3xsin(q_4)}{z_4} \tag{3.23}$$

Similar to the stick jacobian, increase in the bucket angular measurement results in a decrease for the actuator length, z_4. Therefore, a minus sign is introduced in the equation (3.23). Once the cylinder jacobians for each link are calculated, the joint torques can be found using the equation (3.6) above.

4 STATIC ESTIMATION OF THE LOAD WEIGHT

The no-load dynamic torque equations introduced in the equation (3.3) reduce to the equation (4.1) when the machine linkages are stationary, meaning that all the velocity and the acceleration terms are set to zero:

$$\begin{aligned}
\tau_4 &= M_{bu} g r_4 cos(\theta_{234} + \alpha_4) \\
\tau_3 &= \tau_4 + M_{bu} g a_3 cos(\theta_{23}) + M_{st} g r_3 cos(\theta_{23} + \alpha_3) \\
\tau_2 &= \tau_3 + (M_{bu} + M_{st}) g a_2 cos(\theta_2) + M_{bo} r_2 cos(\theta_2 + \alpha_2)
\end{aligned} \tag{4.1}$$

Using the well-known trigonometric identity, $cos(\alpha + \beta) = cos(\alpha)cos(\beta) - sin(\alpha)sin(\beta)$, and writing the equation (4.1) in the decoupled form [34] which is the difference between the torques of two consecutive joints, the equation (4.2) is obtained:

$$\begin{aligned}
\tau_4 &= M_{bu} g r_4 [cos(\theta_{234})cos(\alpha_4) - sin(\theta_{234})sin(\alpha_4)] \\
\tau_{34} = \tau_3 - \tau_4 &= M_{bu} g a_3 cos(\theta_{23}) + M_{st} g r_3 [cos(\theta_{23})cos(\alpha_3) - sin(\theta_{23})sin(\alpha_3)] \\
\tau_{23} = \tau_2 - \tau_3 &= (M_{bu} + M_{st}) g a_2 cos(\theta_2) + M_{bo} g r_2 [cos(\theta_2)cos(\alpha_2) - sin(\theta_2)sin(\alpha_2)]
\end{aligned} \tag{4.2}$$

The equation (4.2) can be written in the matrix form as in the equation (4.3) below:

$$\begin{bmatrix} \tau_4 \\ \tau_{34} \\ \tau_{23} \end{bmatrix} = g \begin{bmatrix} cos(\theta_{234}) & -sin(\theta_{234}) & 0 & 0 & 0 & 0 \\ 0 & 0 & cos(\theta_{23}) & -sin(\theta_{23}) & 0 & 0 \\ 0 & 0 & 0 & 0 & cos(\theta_2) & -sin(\theta_2) \end{bmatrix} \begin{bmatrix} \pi_{s1} \\ \pi_{s2} \\ \pi_{s3} \\ \pi_{s4} \\ \pi_{s5} \\ \pi_{s6} \end{bmatrix} \tag{4.3}$$

The equation (4.3) is in the same form as mentioned in the equation (3.2), with no velocity or acceleration dependency, since the machine linkages are stationary. The vector $\begin{bmatrix} \pi_{s1} & \pi_{s2} & \pi_{s3} & \pi_{s4} & \pi_{s5} & \pi_{s6} \end{bmatrix}^T$ is called gravitational parameter vector and

denoted as π_s and defined in the equation (4.4) below:

$$\pi_s = \begin{bmatrix} \pi_{s1} \\ \pi_{s2} \\ \pi_{s3} \\ \pi_{s4} \\ \pi_{s5} \\ \pi_{s6} \end{bmatrix} = \begin{bmatrix} M_{bu} r_4 cos(\alpha_4) \\ M_{bu} r_4 sin(\alpha_4) \\ M_{bu} a_3 + M_{st} r_3 cos(\alpha_3) \\ M_{st} r_3 sin(\alpha_3) \\ (M_{bu} + M_{st}) a_2 + M_{bo} r_2 cos(\alpha_2) \\ M_{bo} r_2 sin(\alpha_2) \end{bmatrix} \tag{4.4}$$

The method used, that is discussed in the Section 4.2, requires the knowledge of these gravitational parameters introduced in the equation (4.4) in order to predict the no-load torque values and to estimate the load weight in the bucket. Least squares estimation method, that is discussed in the Section 4.3, can be used to estimate the gravitational parameters [21, 33].

There are two unknown gravitational parameters for each torque exerted in the joints as can be seen in the equation (4.3). Therefore, the data of at least two different static postures of the excavator has to be acquired to estimate the gravitational parameters discussed above [27, 34]. However, number of the static postures was increased in the collected data that is discussed in the Section 4.1, in order to compensate the undesired effects like "measurement errors", "static friction", and "minor linkages formed by cylinders" [34].

4.1 Description of collected data

Four different data sets were collected for the static estimation of the load weight in the bucket. The excavator was put in the same static postures with different load weights that are listed below:

- 0 kg, i.e. empty bucket as the training data
- 0 kg, i.e. empty bucket as the test data
- 250 kg as the reference load weight
- 500 kg as the reference load weight

The number of static postures in the data sets are as follows:

- 38 different static postures in the empty bucket for training data
- 19 different static postures in the empty bucket for test data
- 37 different static postures in 250 kg data

- 42 different static postures in 500 kg data

Angular position measurements of the boom, the stick and the bucket linkages were recorded together with the pressure readings of the hydraulic actuators. Therefore, there are three angular position measurements and six pressure readings in each data set.

The training data is used to estimate the gravitational parameters and the test data is used to measure the accuracy of no load torque values that are predicted using the estimated gravitational parameters.

The Figure 4.1 illustrates the angular position measurements of the boom, the stick and the bucket linkages when the bucket is empty for the training data, while the Figure 4.2 displays the test data when the bucket is empty. Also, the Figures 4.3 and 4.4 show the angular position measurements for 250 kg load and 500 kg load, respectively. Notice that the links are kept stationary in different positions in the working space and the angles change at the same time while moving from one stationary pose to the next one.

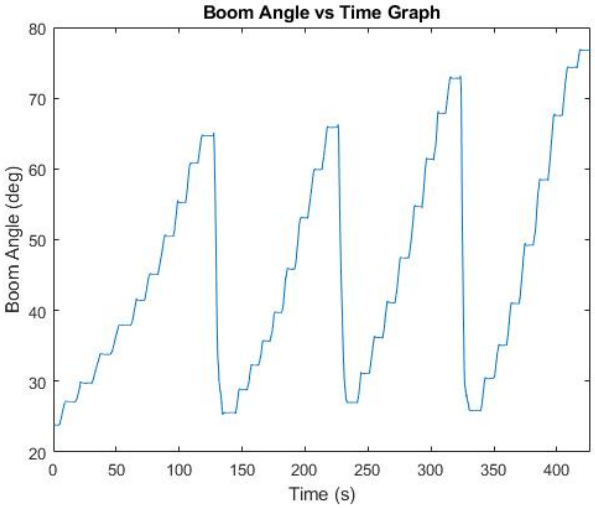

(a) Boom Angle

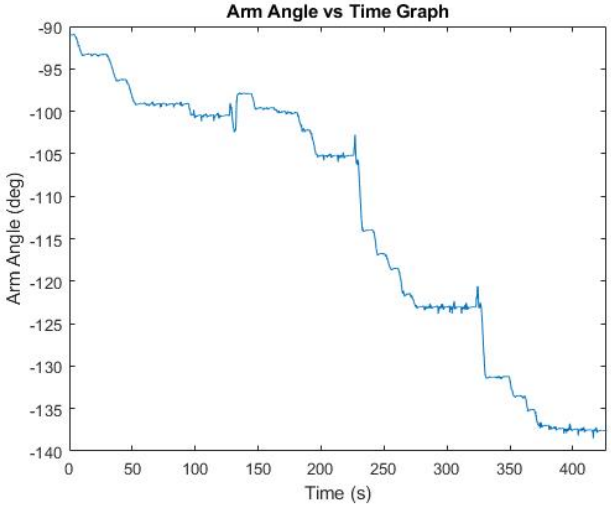

(b) Stick Angle

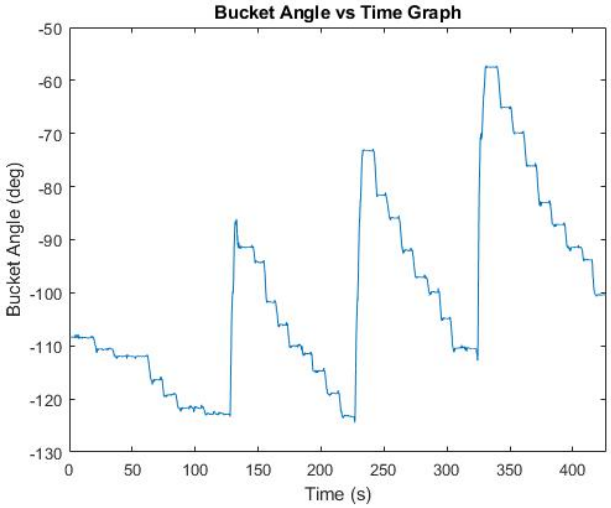

(c) Bucket Angle

Figure 4.1 *Angular position measurements of boom (a), stick (b) and bucket (c) linkages vs time graph for empty bucket, training data with 38 different static calibration points*

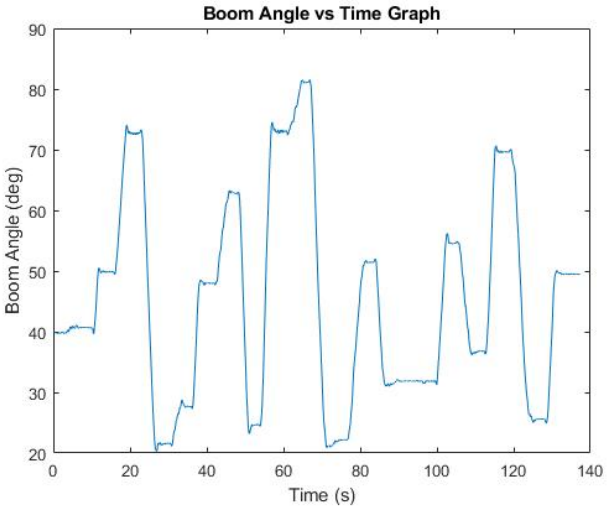

(a) Boom Angle

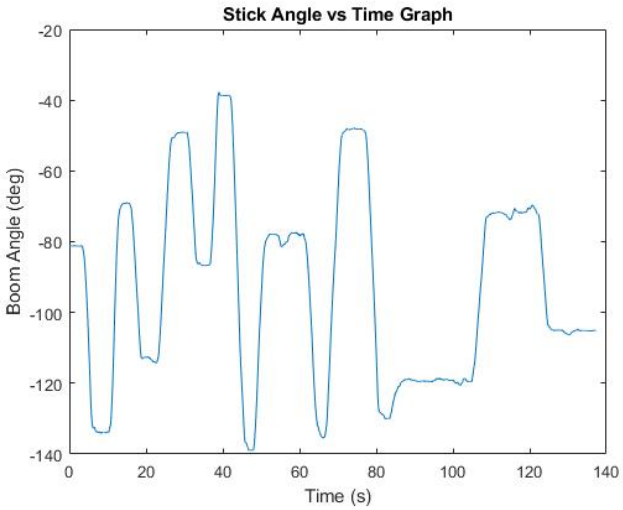

(b) Stick Angle

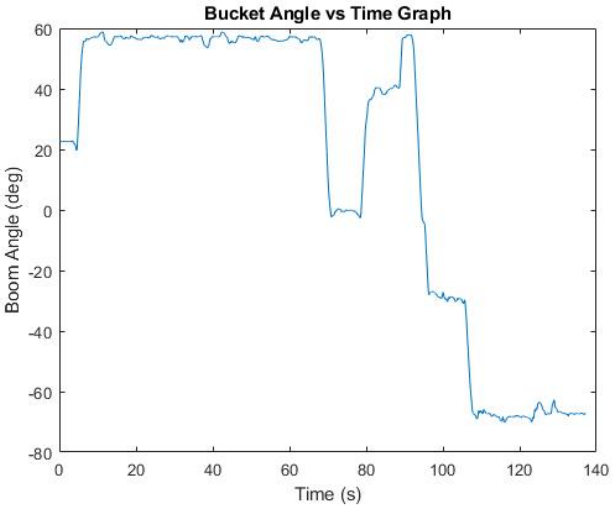

(c) Bucket Angle

Figure 4.2 *Angular position measurements of boom (a), stick (b) and bucket (c) linkages vs time graph for empty bucket, test data with 19 different static postures*

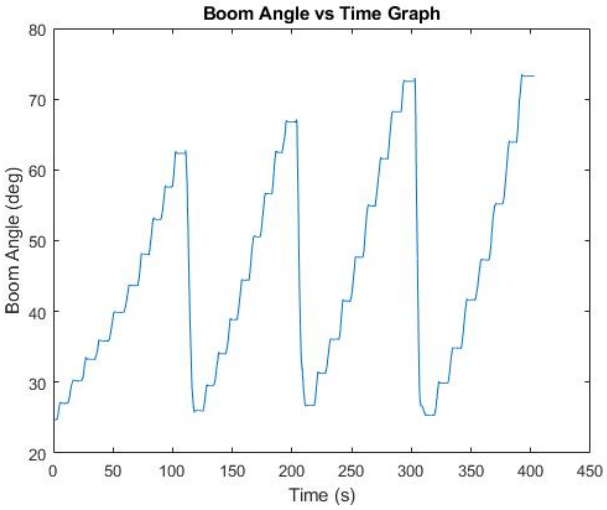

(a) Boom Angle

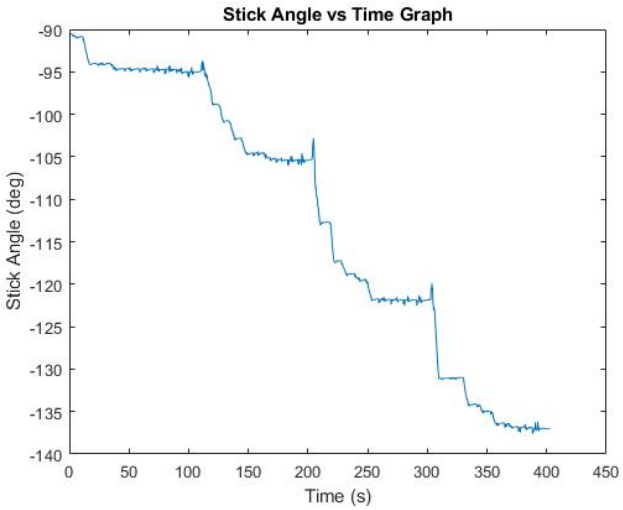

(b) Stick Angle

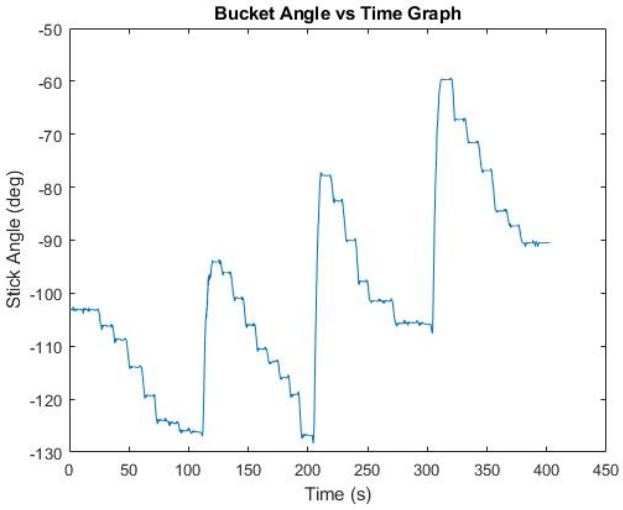

(c) Bucket Angle

Figure 4.3 *Angular position measurements of boom (a), stick (b) and bucket (c) linkages vs time graph for 250 kg data with 37 static postures*

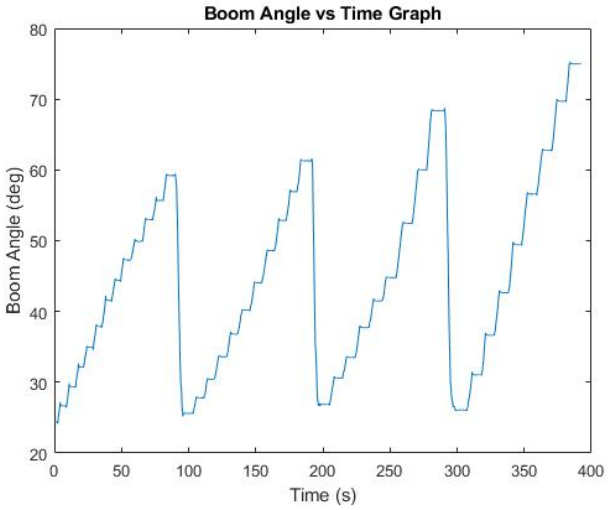

(a) Boom Angle

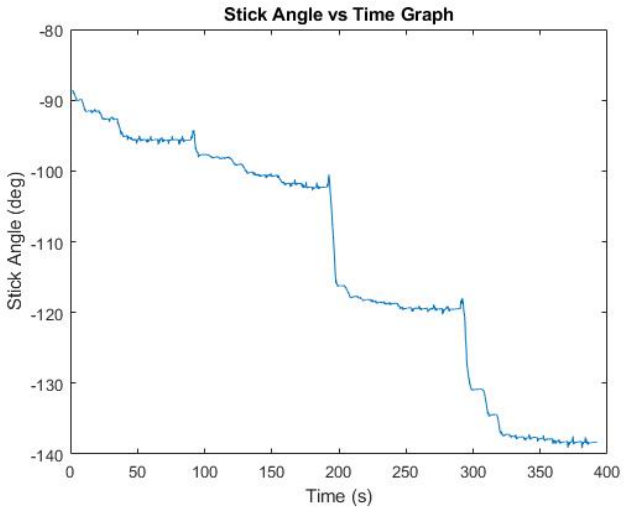

(b) Stick Angle

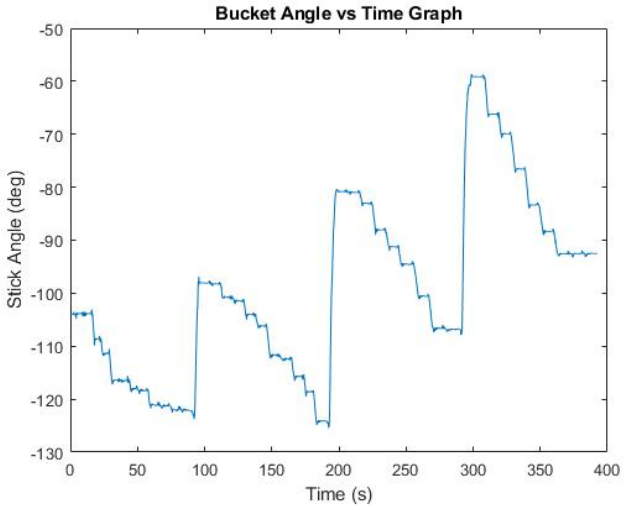

(c) Bucket Angle

Figure 4.4 *Angular position measurements of boom (a), stick (b) and bucket (c) linkages vs time graph for 500 kg data with 42 different static postures*

4.2 Method used in static estimation of the load weight

The torque equations introduced in the Chapter 3 can also be written for the case when the bucket is not empty. Replacing the mass of the bucket, M_{bu}, with $M_{bu}+\hat{M}$, where $\hat{M}$ is the unknown mass of the load, in the equation (4.2) yields the following equation (4.5):

$$\begin{aligned}
\tau_4 &= (M_{bu} + \hat{M})gr_4cos(\theta_{234} + \alpha_4) \\
\tau_{34} &= (M_{bu} + \hat{M})ga_3cos(\theta_{23}) + M_{st}gr_3cos(\theta_{23} + \alpha_3) \\
\tau_{23} &= (M_{bu} + \hat{M} + M_{st})ga_2cos(\theta_2) + M_{bo}r_2cos(\theta_2 + \alpha_2)
\end{aligned} \tag{4.5}$$

The equation (4.5) is valid for any load weight in the bucket and can be written in the form of the equation (4.6) below [32]:

$$\begin{aligned}
\tau_{34_L} &= \tau_{34_{NL}} + \hat{M}ga_3cos(\theta_{23}) \\
\tau_{23_L} &= \tau_{23_{NL}} + \hat{M}ga_2cos(\theta_2)
\end{aligned} \tag{4.6}$$

Where the subscript NL represents the no-load condition and the subscript L corresponds to the loaded bucket condition for the same static posture of the excavator. Solving the equation (4.6) for $\hat{M}$ results in the following equations (4.7) to (4.9) below [32]:

$$\hat{M} = \frac{\tau_{34_L} - \tau_{34_{NL}}}{ga_3cos(\theta_{23})} \tag{4.7}$$

$$\hat{M} = \frac{\tau_{23_L} - \tau_{23_{NL}}}{ga_2cos(\theta_2)} \tag{4.8}$$

$$\hat{M} = \frac{\tau_{24_L} - \tau_{24_{NL}}}{ga_2cos(\theta_2) + ga_3cos(\theta_{23})} \tag{4.9}$$

Where $\tau_{24} = \tau_2 - \tau_4$.

Theoretically, the load weight in the bucket can be estimated using the difference between τ_L and τ_{NL} for the same static posture of the excavator, as stated in the equations (4.7), (4.8) and (4.9). Therefore, there are three methods that can be used to estimate the load weight in the bucket when the links are stationary.

4.2.1 Validation of the method used

In order to make sure that the equations (4.7), (4.8), and (4.9) provide accurate results, the torque values from the collected data were tested. Note that it is not

Table 4.1 *The results of static load weight estimation using the measured torque values for same static postures*

Reference Data	Test Data	Estimated Load Weight	Relative Error (%)
0 kg	250 kg	243.24 kg	2.7
0 kg	500 kg	484.16 kg	3.2

easy to put the machine linkages into same posture with different load weights and 2 degrees of a threshold value is used to identify the similar poses and matching positions from the data sets were evaluated. The results are listed in the Table 4.1.

As can be seen from the results presented in Table 4.1, the load weight in the bucket was estimated with an error which is less than 5% for both test data. Therefore, it can be concluded that the methods proposed in the Section 4.2 can be used to estimate the load weight provided that the data is collected.

The usage of the equations (4.7), (4.8) and (4.9) can be extended. τ_{NL} represents the corresponding no load torque value of a given static posture of the excavator when the bucket is empty, as mentioned earlier. The measurement based no load torque values, τ_{NL}, can be replaced by the predicted torque values, if the gravitational parameters are known. In order to estimate the gravitational parameters, least squares estimation method can be used.

4.3 Estimation of the gravitational parameters

Since each torque equation is described by two gravitational parameters, a multiple linear regression problem has to be solved. The general equation of a multiple regression model with k independent variables is given in the equation (4.10) below [20]:

$$y_i = \beta_0 + \beta_1 x_{i1} + \beta_2 x_{i2} + \cdots + \beta_k x_{ik} + \epsilon_i \tag{4.10}$$

Where y is the dependent variable or response variable, x_1 to x_k are independent variables or the regressors, and ϵ is the error. The matrix notation of the model can be used in order to present the model in a more compact way as written in the equation (4.11) below:

$$y = XB + E$$

Where,

$$y = \begin{bmatrix} y_1 \\ y_2 \\ \vdots \\ y_n \end{bmatrix}, X = \begin{bmatrix} 1 & x_{11} & x_{12} & \dots & x_{1k} \\ 1 & x_{21} & x_{22} & \dots & x_{2k} \\ \vdots & \vdots & & \dots & \\ 1 & x_{n1} & x_{n2} & \dots & x_{nk} \end{bmatrix}, B = \begin{bmatrix} \beta_0 \\ \beta_1 \\ \vdots \\ \beta_k \end{bmatrix}, E = \begin{bmatrix} \epsilon_1 \\ \epsilon_2 \\ \vdots \\ \epsilon_n \end{bmatrix} \tag{4.11}$$

The purpose is to find out the least-squares estimators $\hat{\beta}_0$ to $\hat{\beta}_k$ that minimize the least-squares function $S(B)$, which is given in the equation (4.12) below in the matrix form:

$$S(B) = \sum_{i=1}^{n} \epsilon_i^2 = E^T E = (y - XB)^T (y - XB) \tag{4.12}$$

In order to minimize the least-squares function $S(B)$, the equation (4.13) has to be satisfied by the estimators [20, 30]:

$$X^T X \hat{B} = X^T y \tag{4.13}$$

Therefore, the least-squares estimator of B is given in the equation (4.14) below [20] where the matrix $(X^T X)^{-1} X^T$ called as the "left pseudo-inverse" of X [30]:

$$\hat{B} = (X^T X)^{-1} X^T y \tag{4.14}$$

Recall the equation (4.3), in which τ is the vector of response variables, $Y(\Theta)$ is the regressor and π is the vector of parameters. Note that Y is only the function of angular measurements in static case:

$$Y(\Theta) = g \begin{bmatrix} cos(\theta_{234}) & -sin(\theta_{234}) & 0 & 0 & 0 & 0 \\ 0 & 0 & cos(\theta_{23}) & -sin(\theta_{23}) & 0 & 0 \\ 0 & 0 & 0 & 0 & cos(\theta_2) & -sin(\theta_2) \end{bmatrix} \tag{4.15}$$

Hence, the gravitational parameters are given in the equation (4.16) below:

$$\pi = (Y(\Theta)^T Y(\Theta))^{-1} Y(\Theta)^T \tau \tag{4.16}$$

The gravitational parameters are estimated using the torque values of 38 different static postures in the training data set. The numerical values of the estimated gravitational parameters are given in the Table 4.2 below:

Table 4.2 *Estimated gravitational parameters*

Parameter	Estimated Value (kgm)
π_{s1}	189.85
π_{s2}	318.80
π_{s3}	2753.27
π_{s4}	132.33
π_{s5}	8297.89
π_{s6}	1156.44

Note that all the estimated parameters are positive as expected.

4.4 No-load torque predictions

The purpose of learning the gravitational parameters is to predict the no load torque values for any static configuration of the excavator. The learnt parameters are tested on the data set. As pointed out in the Section 4.1, there are 19 different static postures in the test data.

Since the prediction of the torques is actually a linear regression problem, it is reasonable to calculate the relative error [31]. Therefore, mean absolute percentage error can be used in order to measure the accuracy of the no load torque predictions. Having n as the number of the observations, p_i as the i^{th} prediction and a_i as the actual value of the no load torque for the i^{th} static posture, the equation (4.17) describes how the mean absolute percentage error is calculated [8, 31, 29].

$$MAPE = \frac{100}{n} \sum_{i=1}^{n} \left| \frac{p_i - a_i}{a_i} \right| \tag{4.17}$$

The accuracy of the torque predictions is presented in the Table 4.3 in the sense of mean absolute percentage error.

Table 4.3 *Accuracy of predicted no-load torque values*

Predicted Torque	MAPE
τ_4	40.98%
τ_{34}	10.25%
τ_{23}	8.31%

In the light of the results presented in the Table 4.3, it can be seen that the best predictions are obtained for the difference between the boom torque and the stick torque, τ_{23}, while the worst predictions are obtained for the bucket torque, τ_4. The possible reasons why the prediction error is the highest for the bucket torque are listed below:

- The effect of static friction is more dominant compared to other torque values,

- The test data of the bucket angular measurements exceeds the range of the ones in the training data.

4.5 Load weight estimation with predicted no-load torques

After obtaining all the gravitational parameters required, it is possible to predict the no load torque values for an arbitrary static configuration of the excavator using the equation (4.3). As introduced in the Section 4.2, the load weight in the bucket can be calculated by making use of the estimated no load torque value. However, the bucket torque is predicted with a bad accuracy; therefore, it is decided to proceed with the best prediction, that is the difference between the boom torque and the stick torque, τ_{23}. Hence, the equation (4.8) was selected to be used in the load weight estimation. Note that the equation (4.8) can be written as in the equation (4.18) below by making use of the equation (4.3):

$$\begin{aligned} \hat{M} &= \frac{\tau_{23_L} - \tau_{23_{NL}}}{ga_2 cos(\theta_2)} \\ \tau_{23_{NL}} &= gcos(\theta_2)\pi_{s5} - gsin(\theta_2)\pi_{s6} \\ \hat{M} &= \frac{\tau_{23_L} - gcos(\theta_2)\pi_{s5} + gsin(\theta_2)\pi_{s6}}{ga_2 cos(\theta_2)} \end{aligned} \tag{4.18}$$

Where a_2 is the linear displacement from the boom joint to the stick joint as stated earlier and equals to 4.6m [15]. Load weight estimation was performed using the equation (4.18) over 37 different static postures with 250 kg in the bucket and 42 different static postures with 500 kg in the bucket. As the relative error is measured for the accuracy of the load weight estimation, mean absolute percentage error is used again. The results obtained are presented in the Table 4.4 below:

Table 4.4 *The results of static load weight estimation using the estimated gravitational parameters*

Load Weight	MAPE	Standard Deviation
250 kg	13.98%	13.56%
500 kg	9.42%	6.78%

While the best result for estimation of the 250 kg load is 247.51 kg, the worst result is 381.86 kg. In other words, the values of the absolute percentage error lie between 0.99% and 52.74%. The best estimation result is 501.17 kg for 500 kg load and the worst result is 703.87 kg for the same load, meaning that the value of the absolute percentage error changes from 0.2% to 40.77%. The possible sources of the error are listed below:

- The level of the static friction might be different in different stationary poses of the excavator. Taking the difference between τ_L and τ_{NL} does not completely eliminate the static friction as the friction is not included in the dynamic model and kept outside the scope of this research.

- Accuracy of estimated parameters affect the predicted no load torque values, τ_{NL}. Increasing the number of the static calibration points and covering more parts of the working space of the excavator in the training data set would probably lead to more accurate estimation of gravitational parameters. Thus, more accurate load weight estimation results are going to be obtained.

- The load in the bucket is not uniformly distributed in the bucket. The used reference loads are concrete blocks, and the position of these loads in the bucket might affect the accuracy of the load weight estimation since the measured torque value with the load, τ_{23_L}, in the equation (4.18) may change due to the deviation in the pressure readings.

In order to reduce the error in static load weight estimation, only the configurations, in which the estimation results are accurate enough, should be used.

5 DYNAMIC ESTIMATION OF THE LOAD WEIGHT

When the machine linkages have nonzero velocity or acceleration, each torque equation can be represented by one additional dynamic parameter to the gravitational parameters. Therefore, there are 3 dynamic parameters introduced in total, neglecting the friction. Using the well-known trigonometric identities $cos(\alpha+\beta) = cos(\alpha)cos(\beta) - sin(\alpha)sin(\beta)$ and $sin(\alpha+\beta) = sin(\alpha)cos(\beta) + sin(\alpha)cos(\beta)$, the decoupled version of dynamic torque equations are written in the matrix form that are introduced in the equation (3.3) and the equation (5.1) is obtained. It should be noted that the equation (5.1) is in the form of $\Delta\tau = Y(\Theta, \dot{\Theta}, \ddot{\Theta})\pi$ as shown in the equation (3.2).

$$\Delta\tau = \begin{bmatrix} \tau_4 \\ \tau_{34} \\ \tau_{23} \end{bmatrix}_{3\times1} = \begin{bmatrix} y_{11} & 0 & 0 & y_{14} & y_{15} & 0 & 0 & 0 & 0 \\ 0 & y_{22} & 0 & y_{24} & y_{25} & y_{26} & y_{27} & 0 & 0 \\ 0 & 0 & y_{33} & y_{34} & y_{35} & y_{36} & y_{37} & y_{38} & y_{39} \end{bmatrix}_{3\times9} \begin{bmatrix} \pi_{d1} \\ \pi_{d2} \\ \pi_{d3} \\ \pi_{s1} \\ \pi_{s2} \\ \pi_{s3} \\ \pi_{s6} \\ \pi_{s5} \\ \pi_{s6} \end{bmatrix}_{9\times1} \tag{5.1}$$

Where

$$\begin{aligned}
y_{11} &= \ddot{\theta}_{234} \\
y_{14} &= a_2\ddot{\theta}_2 cos(\theta_{34}) + a_2\dot{\theta}_2^2 sin(\theta_{34}) + a_3\ddot{\theta}_{23}cos(\theta_4) + a_3\dot{\theta}_{23}^2 sin(\theta_4) + gcos(\theta_{234}) \\
y_{15} &= -a_2\ddot{\theta}_2 sin(\theta_{34}) + a_2\dot{\theta}_2^2 cos(\theta_{34}) - a_3\ddot{\theta}_{23}sin(\theta_4) + a_3\dot{\theta}_{23}^2 cos(\theta_4) - gsin(\theta_{234}) \\
y_{22} &= \ddot{\theta}_{23} \\
y_{24} &= a_3\ddot{\theta}_{234}cos(\theta_4) - a_3\dot{\theta}_{234}^2 sin(\theta_4) \\
y_{25} &= -a_3\dot{\theta}_{234}^2 sin(\theta_4) - a_3\dot{\theta}_{234}^2 cos(\theta_4) \\
y_{26} &= a_2\ddot{\theta}_2 cos(\theta_3) + a_2\dot{\theta}_2^2 sin(\theta_3) + gcos(\theta_{23}) \\
y_{27} &= -a_2\ddot{\theta}_2 sin(\theta_3) + a_2\dot{\theta}_2^2 cos(\theta_3) - gsin(\theta_{23}) \\
y_{33} &= \ddot{\theta}_2 \\
y_{34} &= a_2\ddot{\theta}_{234}cos(\theta_{34}) - a_2\dot{\theta}_{234}^2 sin(\theta_{34})
\end{aligned}$$

$$
\begin{aligned}
y_{35} &= -a_2\ddot{\theta}_{234}sin(\theta_{34}) - a_2\dot{\theta}^2_{234}cos(\theta_{34}) \\
y_{36} &= a_2\ddot{\theta}_{23}cos(\theta_3) - a_2\dot{\theta}^2_{23}sin(\theta_3) \\
y_{37} &= -a_2\ddot{\theta}_{23}sin(\theta_3) - a_2\dot{\theta}^2_{23}cos(\theta_3) \\
y_{38} &= gcos(\theta_2) \\
y_{39} &= -gsin(\theta_2)
\end{aligned} \tag{5.2}
$$

It can be seen from the equation (5.1) that one dynamic parameter is introduced for each of the dynamic torque equations as mentioned earlier. The parameter vector π is given in the equation (5.3) below:

$$
\pi = \begin{bmatrix} \pi_{d1} \\ \pi_{d2} \\ \pi_{d3} \\ \pi_{s1} \\ \pi_{s2} \\ \pi_{s3} \\ \pi_{s6} \\ \pi_{s5} \\ \pi_{s6} \end{bmatrix} = \begin{bmatrix} I_{bu} + M_{bu}r_4^2 \\ I + M_{st}r_3^2 + M_{bu}a_3^2 \\ I_{bo} + M_{bo}r_2^2 + (M_{st} + M_{bu})a_2^2 \\ M_{bu}r_4cos(\alpha_4) \\ M_{bu}r_4sin(\alpha_4) \\ M_{bu}a_3 + M_{st}r_3cos(\alpha_3) \\ M_{st}r_3sin(\alpha_3) \\ (M_{bu} + M_{st})a_2 + M_{bo}r_2cos(\alpha_2) \\ M_{bo}r_2sin(\alpha_2) \end{bmatrix} \tag{5.3}
$$

It should be noted that the regressor $Y(\Theta, \dot{\Theta}, \ddot{\Theta})$ includes angular velocity and angular acceleration dependent terms. Since the main purpose of this research is to use only the pressure readings and the angular position measurements in the load weight estimation, the angular velocity and the angular acceleration values were estimated. Even though the collected data that is discussed in the Section 5.1 has the velocity readings from the IMU sensors, the measured angular velocities are used only for checking the accuracy of the estimated velocities. Due to the practical limitations, the angular acceleration values could not be measured. Smoothing splines are used in order to estimate the angular velocity and acceleration values. How the velocity and acceleration values are estimated is discussed in detail in the Section 5.2.

The method used, that is discussed in the Section 5.3, requires the knowledge of the dynamic parameters. Least squares estimation is used in order to estimate the parameters given in the equation (5.3). Estimation of the dynamic parameters is discussed in the Section 5.4.

5.1 Description of collected data

In order to present a generalized weighing algorithm that is independent from the type of the material in the excavator's bucket and reduce the effort needed, contact

of the bucket with the ground is kept outside the scope of this work. Including the interaction of the bucket with the ground would bring additional considerations, such as the force generated by the hydraulic actuators being larger than the resistive force that is exerted by the ground [13, 22] or the fact that the resistive force depends on the soil type that the excavator's bucket is in contact with [2, 13, 23]. Therefore, the followed trajectories were generated on free space in order not to deal with the additional problems mentioned above and to keep the weighing algorithm as simple as possible.

In order to estimate the dynamic parameters appearing in the no load dynamic torque equations, five data sets were collected with different velocities and accelerations. The start point and the end point of the followed trajectories were kept almost the same. However, there are small discrepancies in between the start points and the end points of the trajectories since it is not easy to obtain the same position with different runs of the experiment. One of the five data sets was used to estimate the dynamic parameters and the remaining four data sets were used to measure the accuracy of the predicted no load torque values. Similar trajectories were repeated five times with two different reference loads which are 318 kg and 618 kg. Therefore, 15 data sets were obtained in total. The recorded measurements in each data set are as follows:

- Angular position measurements of the cabin frame, the boom, the stick and the bucket,
- Angular velocity measurements of the boom, the stick and the bucket,
- Pressure readings of hydraulic cylinders.

Since the experiments were performed on a flat ground, the angle of the cabin frame is considered as zero. The plots of the angular position and angular velocity measurements are presented in the Appendix A, and Appendix B, respectively.

5.2 Estimation of angular velocities and angular accelerations

The method used in dynamic estimation of the load weight, that is discussed in the Section 5.3, and estimation of dynamic parameters require the angular velocity and the angular acceleration values, even though there are methods studied in the past that are allowing the parameter identification without using the joint accelerations [11].

Polynomial smoothing splines are used in order to estimate the angular velocity and the angular acceleration values. In order to understand how smoothing splines

work, the definition of spline has to be understood first. A spline is a piece-wise polynomial function of order k that is continuous and has continuous derivatives of order $1, 2, ..., k-1$ at its knots or breakpoints. The knots are points that divide the data to sub-intervals. The degree of the spline is k in each interval and the consecutive polynomials match up at the knots smoothly. Furthermore, derivatives up to $k-2$ also match up at these breakpoints [24]. This property of the splines has been used in estimation of angular velocities and accelerations.

Polynomial smoothing splines have been studied more than five decades and found to be very beneficial for smoothing of noisy data [12, 25, 28]. As the collected data is non-periodic, polynomial curve-fitting technique with a roughness penalty is used in the smoothing splines methodology. Cubic smoothing splines are fitted over the angular position data for the boom, the stick and the bucket. The roughness penalty for a cubic smoothing spline is defined as follows [19]:

$$F(D^2 f) = \int_{min(x)}^{max(x)} \left| D^2 f(t) \right|^2 dt \tag{5.4}$$

The idea is to fit the polynomial to the data that minimizes the equation (5.4) where $min(x)$ and $max(x)$ are the initial and the final time values of the data used.

As the fitted cubic smoothing splines to the angular position data of the boom, the stick and the bucket have continuous first derivatives and second derivatives, it is possible to obtain the estimated angular velocity and angular accelerations. The first derivatives of the smoothing splines are the estimated angular velocities and the second derivatives of the smoothing splines give the estimated angular acceleration values.

Through the process of estimating the angular velocities and angular accelerations, *spaps* [19], *fnder* [17], and *fnval* [18] functions of MATLAB has been used.

Since the angular velocity measurements exist in the collected data as stated in the Section 5.1 for the boom, the stick and the bucket, the accuracy of the estimated angular velocities were measured for each link. After obtaining satisfactory results for the angular velocity predictions, the estimated angular acceleration values are assumed to be correct. The root-mean-squared error values for velocity estimations are given in the Table 5.1 below:

Table 5.1 *Root-mean-squared error values for estimated angular velocities*

Estimated Angular Velocity	RMSE (deg/s)
$\dot{\theta}_2$	0.33
$\dot{\theta}_{23}$	0.35
$\dot{\theta}_{234}$	0.34

The plots of angular velocity estimations and angular acceleration estimations

are shown in the Appendix B and Appendix C, respectively.

5.3 Method used in dynamic estimation of the load weight

The dynamic estimation of the load weight was performed with an assumption that the center of gravity of the bucket is independent from the weight of the load. In other words, the center of gravity of the bucket remains unchanged when the load weight in the bucket changes.

The following decoupled torque equation that is the difference between the boom torque and the stick torque is obtained by replacing M_{bu} with $M_{bu} + \hat{M}$ in the equation (3.3), where $\hat{M}$ is the unknown mass of the load in the bucket:

$$\begin{aligned}\tau_{2_L} - \tau_{3_L} = \tau_{23_L} = {} & [I_{bo} + M_{bo}r_2^2 + (M_{st} + (M_{bu} + \hat{M})a_2^2)]\ddot{\theta}_2 \\ & + M_{st}a_2r_3[\ddot{\theta}_{23}cos(\theta_3 + \alpha_3) - \dot{\theta}_{23}^2 sin(\theta_3 + \alpha_3)] \\ & + (M_{bu} + \hat{M})a_2a_3(\ddot{\theta}_{23}cos(\theta_3) - \dot{\theta}_{23}^2 sin(\theta_3) \\ & + (M_{bu} + \hat{M})a_2r_4[\ddot{\theta}_{234}cos(\theta_{34} + \alpha_4) - \dot{\theta}_{234}^2 sin(\theta_{34} + \alpha_4)] \\ & + (M_{bu} + \hat{M} + M_{st})ga_2cos(\theta_2) + M_{bo}gr_2cos(\theta_2 + \alpha_2) \end{aligned} \quad (5.5)$$

The torque equation (5.5) can be written with the sum of no load torque and the torque value due to the load in the bucket as in the following equation (5.6):

$$\begin{aligned}\tau_{23_L} = {} & \tau_{23_{NL}} + \hat{M}a_2^2\ddot{\theta}_2 + \hat{M}a_2a_3(\ddot{\theta}_{23}cos(\theta_3) - \dot{\theta}_{23}^2 sin(\theta_3)) \\ & + \hat{M}r_4a_2\ddot{\theta}_{234}cos(\theta_{34} + \alpha_4) - \hat{M}r_4a_2\dot{\theta}_{234}^2 sin(\theta_{34} + \alpha_4) + \hat{M}ga_2cos(\theta_2) \end{aligned} \quad (5.6)$$

The equation (5.6) can only be written by assuming that the bucket center of gravity is fixed for an arbitrary value for the load mass $\hat{M}$. In other words, the center of gravity of the bucket remains unchanged when the load weight in the bucket changes. The solution for the unknown load mass $\hat{M}$ is given by the equation (5.7):

$$\hat{M} = \frac{\tau_{23_L} - \tau_{23_{NL}}}{a_2^2y_{33} + r_4cos(\alpha_4)y_{34} + r_4sin(\alpha_4)y_{35} + a_3y_{36} + ga_2cos(\theta_2)} \quad (5.7)$$

Where the parameters y_{33}, y_{34}, y_{35}, and y_{36} are given in the equation (5.2).

The equation (5.7) shows that the unknown load mass in the bucket can be found if the torque values τ_{23_L} and $\tau_{23_{NL}}$ are known over the same trajectory with the same angular velocity and angular acceleration values. It should be noted that the polar coordinates for the center of gravity of the bucket, that are r_4 and α_4 are needed. It is possible to find these parameters if the parameters given in the

equation (5.3) and the mass of the tiltrotator-bucket assembly is known. The mass of the tiltrotator-bucket assembly is reported to be 750 kg, and how the parameters are estimated is explained in detail in the Section 5.4.

5.4 Dynamic parameter estimation

The difference between the boom torque and the stick torque, τ_{23}, is described by seven different parameters as given in the equation (5.1). In addition to the gravitational parameters, one additional dynamic parameter is included in dynamic torque difference between the boom and the stick. Similar to the estimation of gravitational parameters, multiple linear regression problem has to be solved in order to find the seven parameters in discussion.

The difference between the boom torque and the stick torque is given in the equation (5.8) below by making use of the equation (5.1):

$$\tau_{23} = \begin{bmatrix} \ddot{\theta}_2 \\ a_2\ddot{\theta}_{234}cos(\theta_{34}) - a_2\dot{\theta}^2_{234}sin(\theta_{34}) \\ -a_2\ddot{\theta}_{234}sin(\theta_{34}) - a_2\dot{\theta}^2_{234}cos(\theta_{34}) \\ a_2\ddot{\theta}_{23}cos(\theta_3) - a_2\dot{\theta}^2_{23}sin(\theta_3) \\ -a_2\ddot{\theta}_{23}sin(\theta_3) - a_2\dot{\theta}^2_{23}cos(\theta_3) \\ gcos(\theta_2) \\ -gsin(\theta_2) \end{bmatrix}^T \begin{bmatrix} I_{bo} + M_{bo}r_2^2 + (M_{st} + M_{bu})a_2^2 \\ M_{bu}r_4cos(\alpha_4) \\ M_{bu}r_4sin(\alpha_4) \\ M_{bu}a_3 + M_{st}r_3cos(\alpha_3) \\ M_{st}r_3sin(\alpha_3) \\ (M_{bu} + M_{st})a_2 + M_{bo}r_2cos(\alpha_2) \\ M_{bo}r_2sin(\alpha_2) \end{bmatrix} \tag{5.8}$$

Which obeys the linearity of the torque equations with the dynamic parameters, that is already discussed before and given in the equation (5.9) below:

$$\Delta\tau = Y(\Theta, \dot{\Theta}, \ddot{\Theta})\pi \tag{5.9}$$

Where $Y(\Theta, \dot{\Theta}, \ddot{\Theta})$ is the regressor, and π is the vector of parameters. In order to find π, the least squares estimation method is utilized as discussed in the Section 4.3. Therefore, the parameter vector can be found as written in the equation (5.10):

$$\pi = (Y(\Theta, \dot{\Theta}, \ddot{\Theta})^T Y(\Theta, \dot{\Theta}, \ddot{\Theta}))^{-1} Y(\Theta, \dot{\Theta}, \ddot{\Theta})^T \Delta\tau \tag{5.10}$$

The parameter estimation is performed by using a time interval of 10 seconds, i.e. 2000 samples as the system operates at 200 Hz frequency. The estimated parameters are presented in the Table 5.2:

Table 5.2 *Estimated values of parameters appearing in the dynamic torque difference between the boom and the stick*

Parameter	Estimated Value
π_{d3}	28827.71 kgm^2
π_{s1}	298.04 kgm
π_{s2}	592.86 kgm
π_{s3}	8228.37 kgm
π_{s4}	2571.05 kgm
π_{s5}	8927.32 kgm
π_{s6}	1386.54 kgm

Note that all the estimated parameters are positive as expected. The discrepancy between the results for the gravitational parameters that are presented in the Table 4.2 and the results of the dynamic identification that are given in the Table 5.2 is believed to be caused by the existence of the static friction in the estimation of gravitational parameters that is discussed in the Section 4.3.

5.4.1 Polar coordinates of bucket's center of gravity

If the mass of tiltrotator-bucket assembly is known, the polar coordinates of the bucket's center of gravity can be calculated. Recall the parameter vector of the dynamic torque equation that gives the difference between the boom torque and the stick torque:

$$\pi = \begin{bmatrix} I_{bo} + M_{bo}r_2^2 + (M_{st} + M_{bu})a_2^2 \\ M_{bu}r_4 cos(\alpha_4) \\ M_{bu}r_4 sin(\alpha_4) \\ M_{bu}a_3 + M_{st}r_3 cos(\alpha_3) \\ M_{st}r_3 sin(\alpha_3) \\ (M_{bu} + M_{st})a_2 + M_{bo}r_2 cos(\alpha_2) \\ M_{bo}r_2 sin(\alpha_2) \end{bmatrix} \tag{5.11}$$

One can obtain the angle value α_4 by dividing the third element of the vector π by the second element and then taking the inverse tangent of the result as given in the equation (5.12).

$$\alpha_4 = tan^{-1}\left(\frac{\pi_{s2}}{\pi_{s1}}\right) \tag{5.12}$$

Then, the parameter r_4 can be solved by using one of the following relations given in the equation (5.13) below:

$$r_4 = \frac{\pi_{s1}}{M_{bu} cos(\alpha_4)}$$
$$r_4 = \frac{\pi_{s2}}{M_{bu} sin(\alpha_4)} \tag{5.13}$$

Estimating the values for polar coordinates of bucket's center of gravity, α_4 and r_4, using the equations (5.12) and (5.13), makes it possible to estimate the load weight by using the equation (5.7).

5.5 Validation of the method used

The method developed in the Section 5.3 was tested over three different scenarios. As stated in the Section 5.1, the collected data consists of the information regarding the 0 kg load, i.e. the empty bucket, 318 kg load and 618 kg load. The following Table 5.3 shows the outcomes of the load weight estimation that is performed using the measured torque values with and without the load in the equation (5.7).

Table 5.3 *The results of dynamic load weight estimation using the measured torque values*

Reference Data	Test Data	Estimated Load Weight	Error(%)
0 kg	318 kg	332.07 kg	4.42%
0 kg	618 kg	653.66 kg	5.77%
318 kg	618 kg	319.41 kg	6.47%

The tests are performed over 5 seconds of time intervals, i.e. 1000 samples were used. The load weight estimation was performed for each sample that is used and an array of estimated mass was generated. Finally, the mean value of the 1000 mass estimations is presented as the result. The results obtained using the collected data itself resulted in an error of 5% in average as shown in the Table 5.3, which is quite accurate and the assumption for the fixed center of gravity of the bucket seemed to be working. It should be noted that it is very difficult to follow the same trajectory with the same velocity and acceleration values with a human-operated excavator. Also, the accuracy of the predicted angular velocity and angular acceleration values affect the result of the load weight estimation. Moreover, the friction plays a role as a source of the error in the estimated load weight.

The usage of the equation (5.7) can be extended as done in the static load weight estimation by replacing the measurement based no load torque values, $\tau_{23_{NL}}$, with the predicted no load torque values, $\tau_{\hat{23}_{NL}}$. The predicted no load torque values for the angular position, velocity and acceleration of the links when the bucket is loaded can be found by making use of the estimated parameters that are listed in the Table

5.2 and the equation (5.8). Therefore, the load weight can be estimated by using the difference between the measured torque value with the load, and the predicted no-load torque value for the same angular position, velocity and acceleration values.

5.6 No load dynamic torque predictions & accuracy

The no load torque value, $\tau_{23_{NL}}$, can be predicted for any angular position, angular velocity, and angular acceleration by using the equation (5.8) since the parameters are estimated. Then, the corresponding no load torque value can be estimated over any trajectory that the machine links follow when the bucket is not empty, and for the same angular velocity and acceleration values.

As described in the Section 5.1, there are five different data sets for empty bucket case. Remember that one of these data sets were used to estimate the parameters that describe the no load torque difference between the boom and the stick, $\tau_{23_{NL}}$. The other four data sets were used to test the accuracy of the predicted torque values by making use of the estimated parameters. The following Table 5.4 shows the mean absolute percentage error of the predicted torque values and the Figure 5.1 presents a comparison between the actual torque values and the predicted torque values when the bucket is empty.

Table 5.4 *Accuracy of predicted dynamic no-load torque values*

Predicted $\tau_{23_{NL}}$	MAPE
Data set #1	4.20%
Data set #2	5.24%
Data set #3	5.67%
Data set #4	3.85%

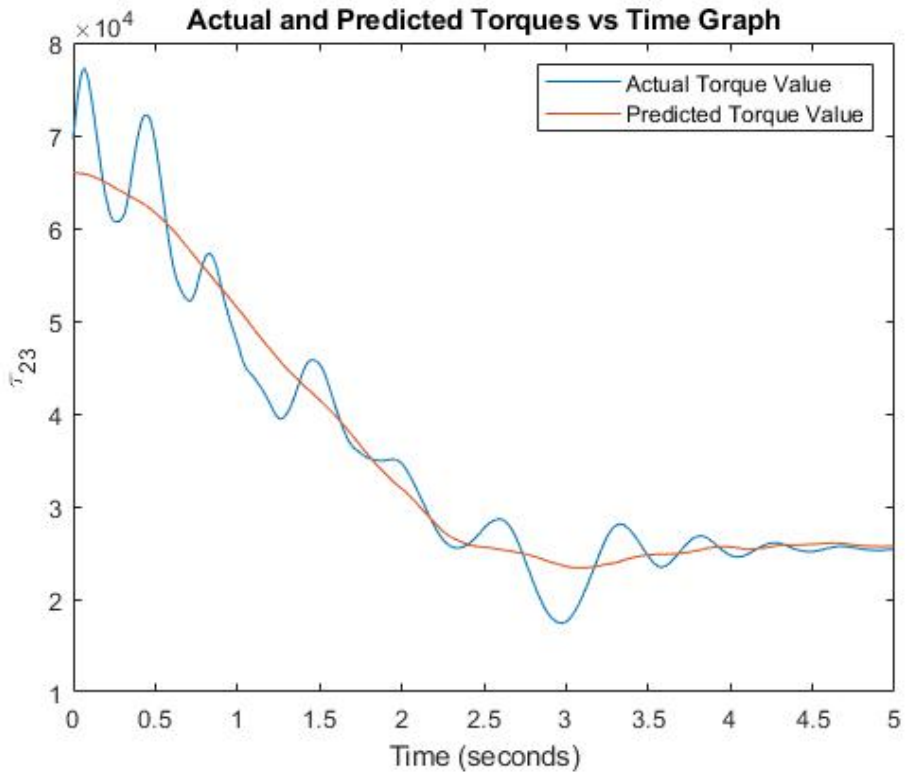

Figure 5.1 *Actual and predicted torque differences between the boom and the stick*

5.7 Load weight estimation with predicted no-load torques

The method proposed in the Section 5.3 uses the difference between the loaded torque values (τ_{23_L}) and no load torque values ($\tau_{23_{NL}}$) of the difference between the boom torque and the stick torque. It is possible to replace the measured no load torque difference between the boom and the stick, $\tau_{23_{NL}}$, with the predicted value, $\hat{\tau}_{23_{NL}}$, as the estimated parameters serve well in predicting the no load torque values. Therefore, it is possible to estimate the load weight in the bucket by calculating the loaded torque value and predicting the corresponding no load torque value over the same trajectory with the same angular velocity and angular acceleration values, as represented in the equation (5.14) below:

$$\hat{M} = \frac{\tau_{23_L} - \hat{\tau}_{23_{NL}}}{a_2^2 y_{33} + r_4 cos(\alpha_4) y_{34} + r_4 sin(\alpha_4) y_{35} + a_3 y_{36} + g a_2 cos(\theta_2)} \tag{5.14}$$

Where the parameters y_{33}, y_{34}, y_{35}, and y_{36} are given in the equation (5.2).

Three different scenarios were generated to test how accurate the method works with the predicted no load torque values by making use of the estimated parameters. These scenarios are listed below:

- Load weight estimation over five seconds of time intervals where the excava-

tor's links have high angular velocities e.g. 2 deg/s.

- Load weight estimation over only the dynamic parts of the data sets. In other words, the parts of data sets in which the links of the excavator are stationary are discarded.
- Load weight estimation by making use of all the samples in the data set.

The results of the load weight estimation for these three different scenarios are presented in the Tables 5.5, 5.6, and 5.7, respectively.

Table 5.5 *The results of dynamic load weight estimation over 5 seconds of time intervals*

Test Data	Estimated Load Weight	Error (%)
Data set #1, 618 kg	614.22 kg	0.61%
Data set #2, 618 kg	612.39 kg	0.91%
Data set #3, 618 kg	610.89 kg	1.15%
Data set #4, 618 kg	623.53 kg	0.90%
Data set #5, 618 kg	621.33 kg	0.54%
Data set #1, 318 kg	319.24 kg	0.39%
Data set #2, 318 kg	313.99 kg	1.26%
Data set #3, 318 kg	317.19 kg	0.26%
Data set #4, 318 kg	321.68 kg	1.16%
Data set #5, 318 kg	332.69 kg	4.62%

The mean value of the error is 0.82% and the standard deviation is 0.25% for estimation of 618 kg load. The mean value of the error is 1.54% and the standard deviation is 1.78% for estimation of 318 kg load.

Table 5.6 *The results of dynamic load weight estimation using only the dynamic parts of the data sets*

Test Data	Estimated Load Weight	Error (%)
Data set #1, 618 kg	630.77 kg	2.07%
Data set #2, 618 kg	642.37 kg	3.94%
Data set #3, 618 kg	621.90 kg	0.63%
Data set #4, 618 kg	606.41 kg	1.87%
Data set #5, 618 kg	612.75 kg	0.85%
Data set #1, 318 kg	336.17 kg	5.71%
Data set #2, 318 kg	310.63 kg	2.32%
Data set #3, 318 kg	310.84 kg	2.25%
Data set #4, 318 kg	349.36 kg	9.86%
Data set #5, 318 kg	323.26 kg	1.65%

The mean value of the error is 1.87% and the standard deviation is 1.31% for estimation of 618 kg load. The mean value of the error is 4.36% and the standard deviation is 3.47% for estimation of 318 kg load.

Table 5.7 *The results of dynamic load weight estimation using all the samples in the data sets*

Test Data	Estimated Load Weight	Error (%)
Data set #1, 618 kg	618.87 kg	0.14%
Data set #2, 618 kg	510.55 kg	17.39%
Data set #3, 618 kg	603.33 kg	2.37%
Data set #4, 618 kg	567.38 kg	8.19%
Data set #5, 618 kg	541.41 kg	12.39%
Data set #1, 318 kg	279.24 kg	12.19%
Data set #2, 318 kg	298.28 kg	6.20%
Data set #3, 318 kg	290.09 kg	8.78%
Data set #4, 318 kg	340.66 kg	7.13%
Data set #5, 318 kg	301.64 kg	5.15%

The mean value of the error is 8.10% and the standard deviation is 7.09% for estimation of 618 kg load. The mean value of the error is 7.89% and the standard deviation is 2.75% for estimation of 318 kg load.

It can be observed from the results presented in the Tables 5.5, 5.5, 5.5 that the best results are obtained when the links have at least 2 deg/s velocity. Also, the worst results were obtained by inclusion of stationary parts of the data to the method proposed. The possible reasons for the error are listed below:

- The assumption that the center of gravity of the bucket is fixed is not correct.
- The accuracy of the estimated angular velocities and angular accelerations
- The friction
- Measurement errors caused by the sensors

6 CONCLUSIONS

This thesis proposes methods for load weight estimation on excavators by using only the angular position measurements of the excavator's links and pressure readings in the hydraulic cylinders. The load weight estimation problem is divided into two cases that are the static estimation and the dynamic estimation of the load weight in the excavator's bucket. The static estimation is an existing approach that is tested on a mini excavator [34]. The results obtained served as a good starting point and the method used in static estimation is tested using two different reference load masses that are 250 kg and 500 kg. Afterwards, the approach is extended to the dynamic load weight estimation with an assumption that the bucket's center of gravity is fixed. In order to utilize the methods in both the static estimation and dynamic estimation, a parameter estimation problem had to be solved. Only the gravitational parameters are estimated in the static estimation and one additional dynamic parameter is estimated in the dynamic estimation. The discrepancies resulted in the estimation of gravitational parameters are discussed. Also, the angular velocities and angular accelerations had to be estimated in order to make use of the method that is proposed for the dynamic load weight estimation. A curve fitting approach is used to estimate the angular velocities and angular accelerations by making use of the smoothing splines on the angular position measurements. Angular velocities and angular accelerations are estimated based on the derivatives of the piece-wise polynomial functions that are fitted on the angular position measurements.

The method developed for the dynamic load weight estimation is tested over two different reference load masses that are 318 kg and 618 kg. Three different scenarios are generated and the results for each scenario are discussed in detail. The results that are obtained showed that the dynamic load weight estimation gives quite accurate results that are less than 2% when the excavator's links have high enough velocity values, e.g. at least 2 deg/s. Also, the worst results are obtained when the data of the stationary poses of the excavator is taken into account. Finally, the possible sources of the errors in the load weight estimation for both static and dynamic cases are presented.

7 FUTURE WORK

The methods proposed for static estimation and dynamic estimation of the load weight are evaluated as an offline manner. As a further step, the methods that are developed can be tested online on the real excavator and the results can be observed.

Collecting more data with more stationary calibration points would result in more accurate gravitational parameter estimation; therefore, more accurate stationary no load torque values could be obtained. As a result, the error of the predicted load weight in static estimation would decrease. Furthermore, the friction is not included in this study, as stated earlier. However, there are existing research that also model the friction and calculate the torque values accordingly. Inclusion of a model regarding the static friction would bring a significant improvement in the static load weight estimation.

The actual values of angular velocities and angular accelerations can be used instead of the estimated angular velocities and the estimated angular accelerations, since the used IMU sensors, that are developed by Novatron Oy, provide the angular acceleration measurements. Also, the dynamic friction, or kinetic friction, can be modeled and included in the dynamic load weight estimation. Thus, more accurate predictions for the load weight can be obtained.

REFERENCES

[1] Frederic Ballaire. “Dynamic, continuous, and center of gravity independent weighing with a loader”. PhD thesis. Technical University of Kaiserslautern, 2015.

[2] Nureddin Bennett, Ashwin Walawalkar, Meike Hack, and Christian Schindler. “Integration of digging forces in a multi-body-system model of an excavator”. In: *Proceedings of the Institution of Mechanical Engineers, Part K: Journal of Multibody Dynamics* 230 (June 2015).

[3] Ernest F. Brater, Horace W. King, James E. Lindell, and C. Y. Wei. *Handbook of Hydraulics*. 6th ed. McGraw-Hill, 1996.

[4] Yunfei Dong, Tianyu Ren, Ken Chen, and Dan Wu. “An efficient robot payload identification method for industrial application”. In: *Industrial robot* 45.4 (2018), pp. 505–515.

[5] M. Gautier, W. Khalil, C. Presse, and P.P Restrepo. “Experimental identification of dynamic parameters of robot”. In: *IFAC Proceedings Volumes* 27.14 (1994), pp. 625–630.

[6] Artur Gawlik and Piotr Kucybała. “Dynamic Weighing System Used in Excavator”. In: *Journal of KONES* 24.4 (2017), pp. 31–38.

[7] Claudio Gaz and Alessandro De Luca. “Payload estimation based on identified coefficients of robot dynamics — With an application to collision detection”. In: *2017 IEEE/RSJ International Conference on Intelligent Robots and Systems (IROS)*. 2017, pp. 3033–3040.

[8] Mustafa Göçken, Mehmet Özçalıcı, Aslı Boru, and Ayşe Tuğba Dosdoğru. “Integrating metaheuristics and Artificial Neural Networks for improved stock price prediction”. In: *Expert Systems With Applications* 44 (Feb. 2016), pp. 320–331.

[9] N. G. Hareesha and K. N. Umesh. “Kinematic and Isotropic Properties of Excavator Mechanism”. In: July 2018.

[10] Jahmy J. Hindman. “Dynamic payload estimation in four wheel drive loaders”. PhD thesis. University of Saskatchewan, 2008.

[11] Ping Hsu, M. Bodson, S. Sastry, and B. Paden. “Adaptive identification and control for manipulators without using joint accelerations”. In: *IEEE Int. Conf. Robot. Automat.* Vol. 4. 1987, pp. 1210–1215.

[12] M. F. Hutchinson and F. R. de Hoog. “Smoothing Noisy data with spline Functions”. In: *Numerische Mathematik* 47 (Mar. 1985), pp. 99–106.

[13] Y. Khedkar, T. Dey, and Y. Padasalagi. “Study of Forces Acting on Excavator Bucket While Digging”. In: *Journal of Applied Mechanical Engineering* 06 (Jan. 2017).

[14] P. K. Khosla and T. Kanade. “Parameter identification of robot dynamics”. In: *1985 24th IEEE Conference on Decision and Control*. 1985, pp. 1754–1760.

[15] *Komatsu PC138US-8 Hydraulic Excavator Datasheet*. Komatsu.

[16] Ziren Lu, Karunakar B. Shimoga, and Andrew A. Goldenberg. “Experimental determination of dynamic parameters of robotic arms”. In: *Journal of Robotic Systems* 10.8 (1993), pp. 1009–1029.

[17] *MATLAB Documentation fnder*. `https://se.mathworks.com/help/curvefit/fnder.html`. Accessed: 2020-04-02.

[18] *MATLAB Documentation fnval*. `hhttps://se.mathworks.com/help/curvefit/fnval.html`. Accessed: 2020-04-02.

[19] *MATLAB Documentation spaps*. `https://se.mathworks.com/help/curvefit/spaps.html`. Accessed: 2020-04-02.

[20] Douglas C. Montgomery, Elizabeth A. Peck, and G. Geoffrey Vining. “Introduction to Linear Regression Analysis”. In: 5th ed. Wiley, 2012. Chap. 3.

[21] N. R. Parker, S. E. Salcudean, and P. D. Lawrence. “Application of force feedback to heavy duty hydraulic machines”. In: *IEEE Int. Conf. Robot. Automat.* May 1993, pp. 375–381.

[22] Bhaveshkumar P. Patel and J. M Prajapati. “Evaluation of bucket capacity, digging force calculation and static force analysis of mini hydraulic backhoe excavator”. In: *Machine Design: The Journal of Faculty of Technical Sciences* 4 (Apr. 2012), pp. 59–66.

[23] Bhaveshkumar P. Patel and J. M Prajapati. “Evaluation of Resistive Force using Principle of Soil Mechanics for Mini Hydraulic Backhoe Excavator”. eng. In: *International journal of machine learning and computing* (2012), pp. 386–391. ISSN: 2010-3700.

[24] J. O. Ramsay and B.W. Silverman. “Functional Data Analysis”. In: Springer, 2005. Chap. 3.

[25] Christian H. Reinsch. “Smoothing by spline functions”. In: *Numerische Mathematik* 10 (1967), pp. 77–183.

[26] Anton Renner, Hannes Wind, and Oliver Sawodny. “Online payload estimation for hydraulically actuated manipulators”. In: *Mechatronics* 66 (2020), p. 102322.

[27] S. E. Salcudean, S. Tafazoli, P. D. Lawrence, and I. Chau. “Impedance control of a teleoperated mini excavator”. In: *IEEE Int. Conf. Adv. Robot.* Monterey,CA,USA, July 1997, pp. 19–25.

[28] I. J Schoenberg. “Spline functions and the problem of graduation”. In: *Proceedings of the National Academy of Sciences - PNAS* 52.4 (1964), pp. 947–950.

[29] Maxim Shcherbakov, Adriaan Brebels, N.L. Shcherbakova, Anton Tyukov, T.A. Janovsky, and V.A. Kamaev. “A survey of forecast error measures”. In: *World Applied Sciences Journal* 24 (Jan. 2013), pp. 171–176.

[30] Bruno Siciliano, Lorenzo Sciavicco, Luigi Villani, and Giuseppe Oriolo. “Robotics Modelling, Planning and Control”. In: Springer, 2009. Chap. 7.

[31] David A. Swanson, Jeff Tayman, and T. M. Bryan. “MAPE-R: A rescaled measure of accuracy for cross-sectional subnational population forecasts”. In: *Journal of Population Research* 28 (Mar. 2011), pp. 225–243.

[32] S. Tafazoli, P. D. Lawrence, S. E. Salcudean, D. Chan, S. Bachmann, and C. W. de Silva. “Parameter estimation and actuator friction analysis for a mini excavator”. In: *IEEE Int. Conf. Robot. Automat.* Minneapolis,MN,USA, Apr. 1996, pp. 329–334.

[33] Shahram Tafazoli. “Identification of frictional effects and structural dynamics for improved control of hydraulic excavators”. PhD thesis. University of British Columbia, 1997.

[34] Shahram Tafazoli, Peter. D. Lawrence, and S.E. Salcudean. “Identification of inertial and friction parameters for excavator arms”. In: *IEEE Transactions on Robotics and Automation* 15.5 (Oct. 1999), pp. 966–971.

[35] Ashwin Walawalkar, S. Heep, Martin Frank, R. Leifeld, and Christian Schindler. “Validation of an analytical method for payload estimation in excavators”. In: *Commercial Vehicle Technology 2018*. Mar. 2018.

[36] Ashwin Walawalkar, Steffen Heep, Florian Schneider, Jan Schüßler, and Christian Schindler. “A method for payload estimation in excavators”. In: *Proceedings of the 4th Commercial Vehicle Symposium* (2016), pp. 424–437.

[37] Seungjin Yoo, Cheol-Gyu Park, and Seung-Han You. “Inertial parameter estimation for the dynamic simulation of a hydraulic excavator”. In: *Journal of Mechanical Science and Technology* 32.9 (2018), pp. 4045–4056.

[38] Yahya H. Zweiri. “Identification schemes for unmanned excavator arm parameters”. In: 5.2 (2008), pp. 185–192.

A VISUALIZATION OF ANGULAR POSITION MEASUREMENTS IN DYNAMIC LOAD WEIGHT ESTIMATION

The angular position measurements and estimations from the boom, the stick and the bucket links are plotted in this appendix for all the data sets collected for dynamic load weight estimation. The tolerance values used in the function *spaps* are 5.1×10^{-4}, 5.5×10^{-4}, and 5.2×10^{-4} for the boom, the stick, and the bucket, respectively.

A.1 Angular position graphs for data sets with empty bucket

This section provides the angular position graphs for the data sets with empty bucket. The following Figures A.1, A.2, A.3, A.4, and A.5 represent the boom, the stick, and the bucket angular position measurements together with the fitted polynomials using smoothing splines as described in Section 5.2.

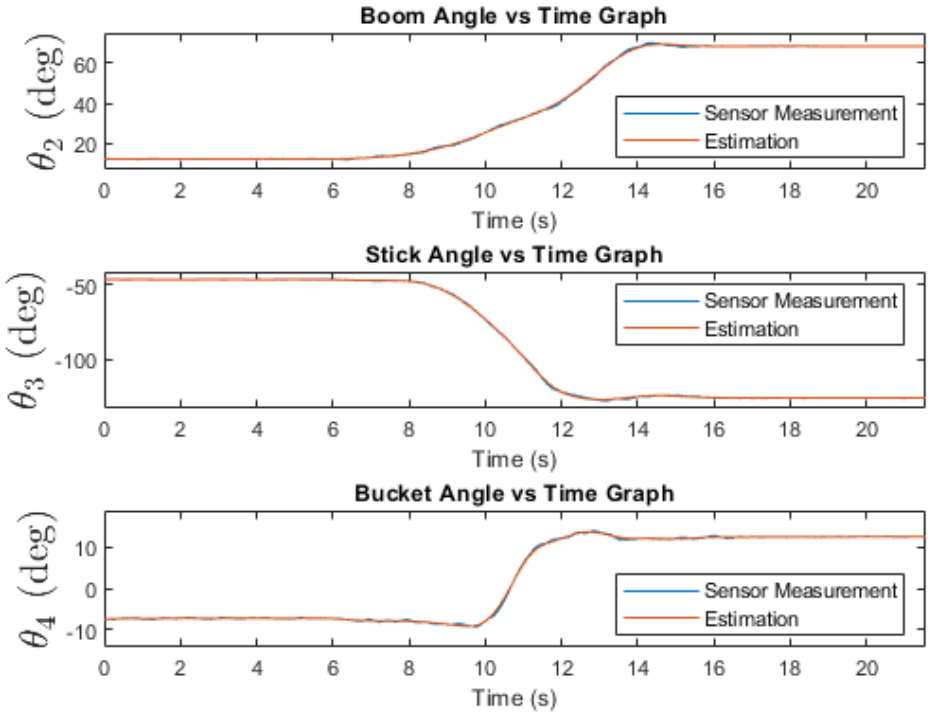

Figure A.1 *Angular position measurements and estimations, data set 1, empty bucket*

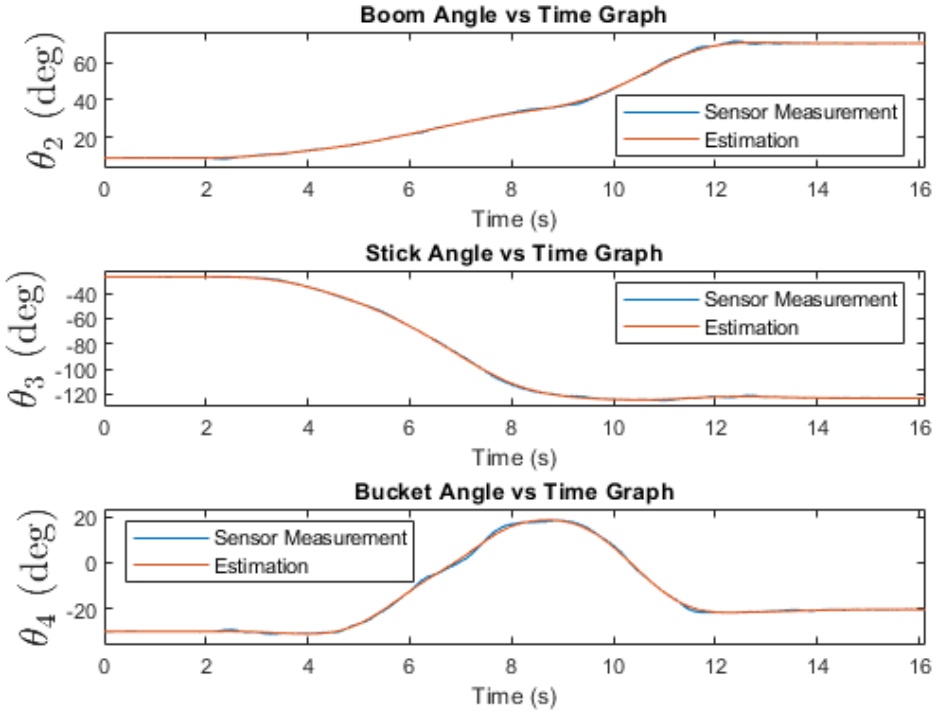

Figure A.2 *Angular position measurements and estimations, data set 2, empty bucket*

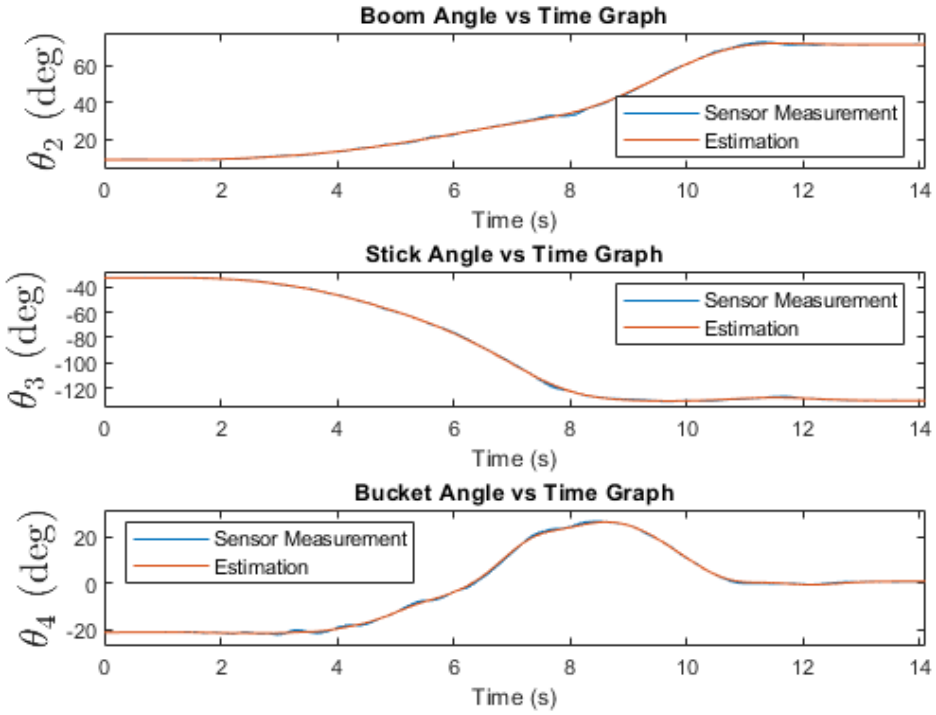

Figure A.3 *Angular position measurements and estimations, data set 3, empty bucket*

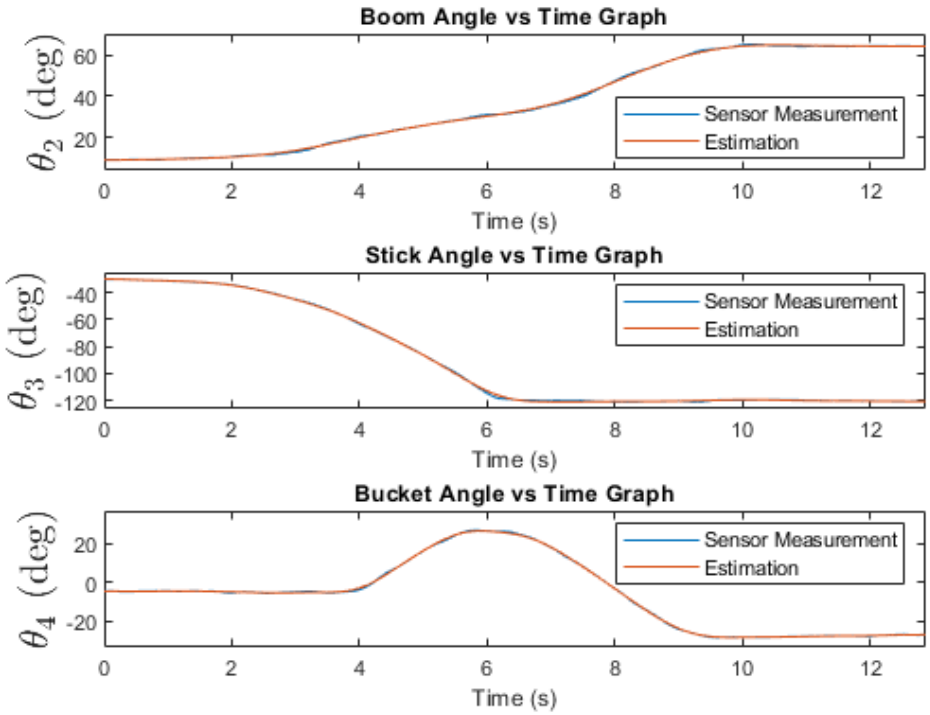

Figure A.4 *Angular position measurements and estimations, data set 4, empty bucket*

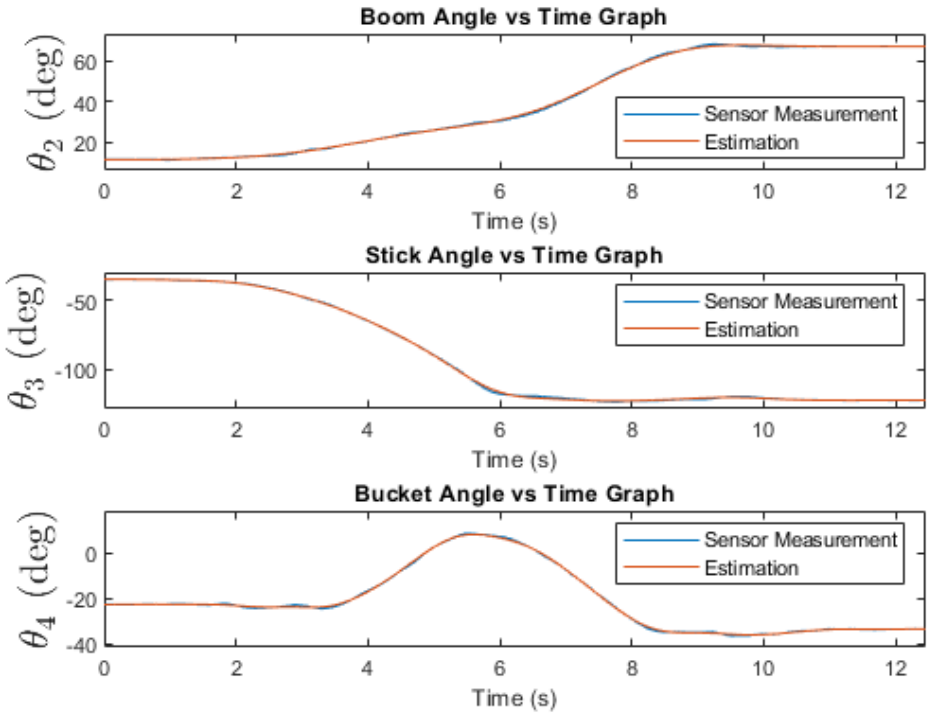

Figure A.5 *Angular position measurements and estimations, data set 5, empty bucket*

A.2 Angular position graphs for data sets with 318 kg reference load

The angular position graphs for the data sets with 318 kg reference load in the bucket are presented in this section. The following Figures A.6, A.7, A.8, A.9, and A.10 illustrate the boom, the stick, and the bucket angular position measurements and the estimated position values using smoothing splines as stated in Section 5.2.

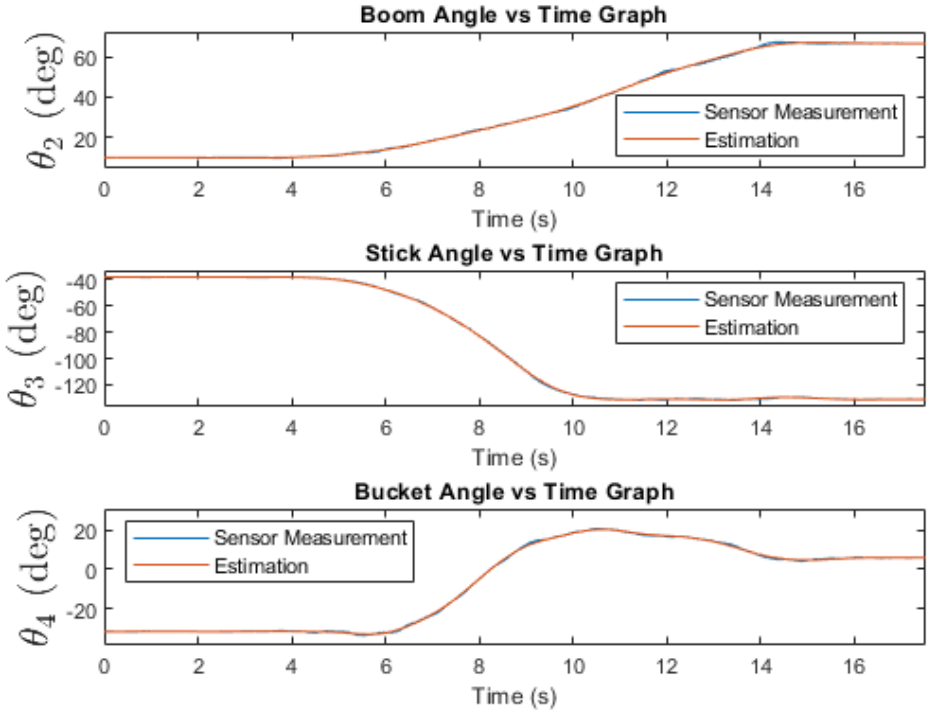

Figure A.6 *Angular position measurements and estimations, data set 1, 318 kg load*

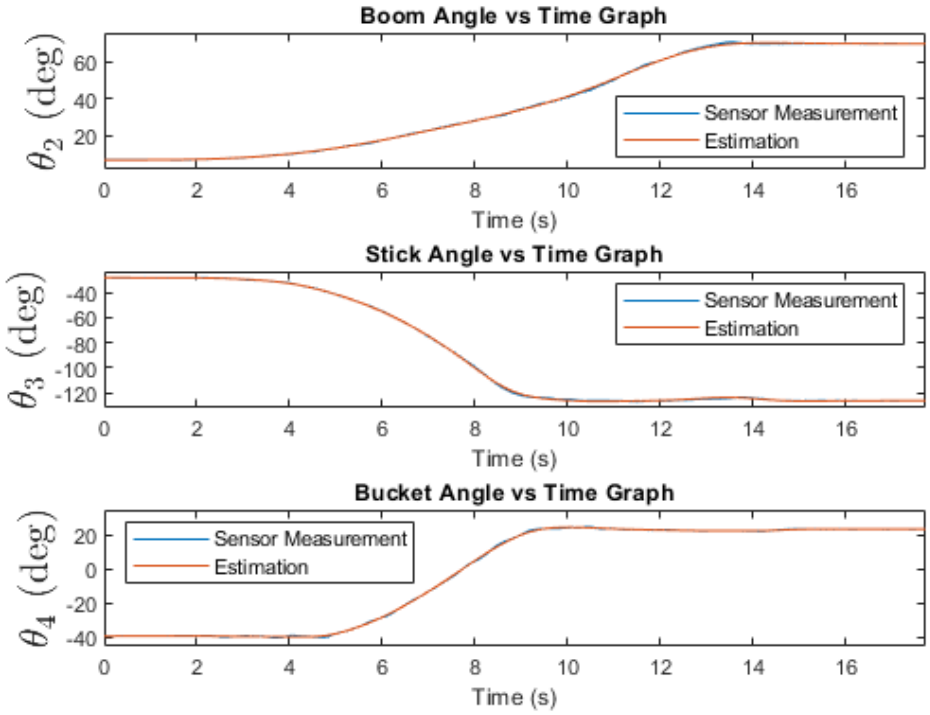

Figure A.7 *Angular position measurements and estimations, data set 2, 318 kg load*

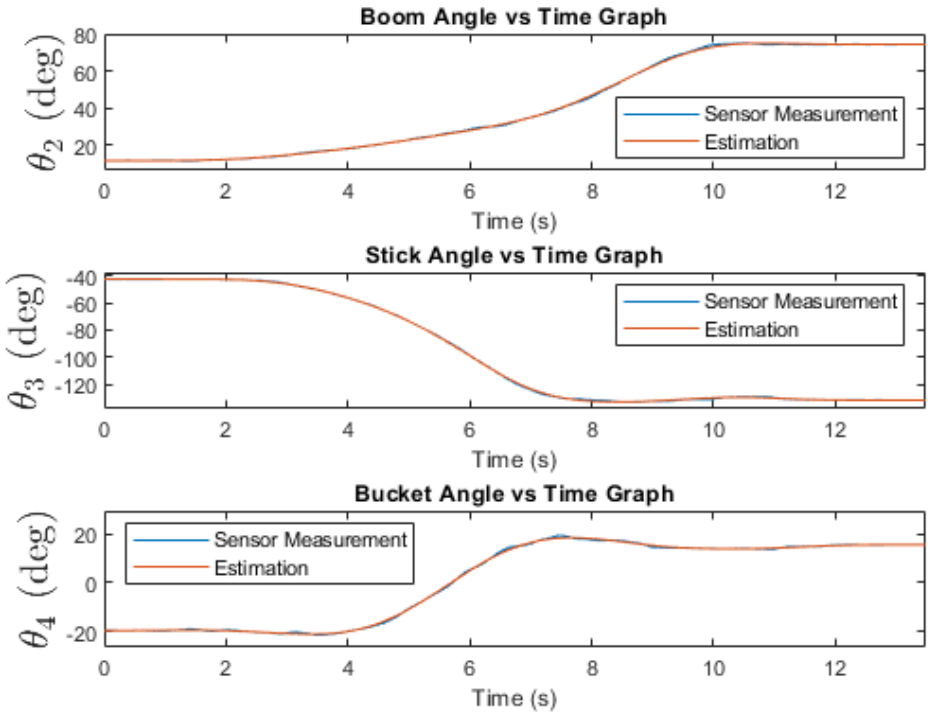

Figure A.8 *Angular position measurements and estimations, data set 3, 318 kg load*

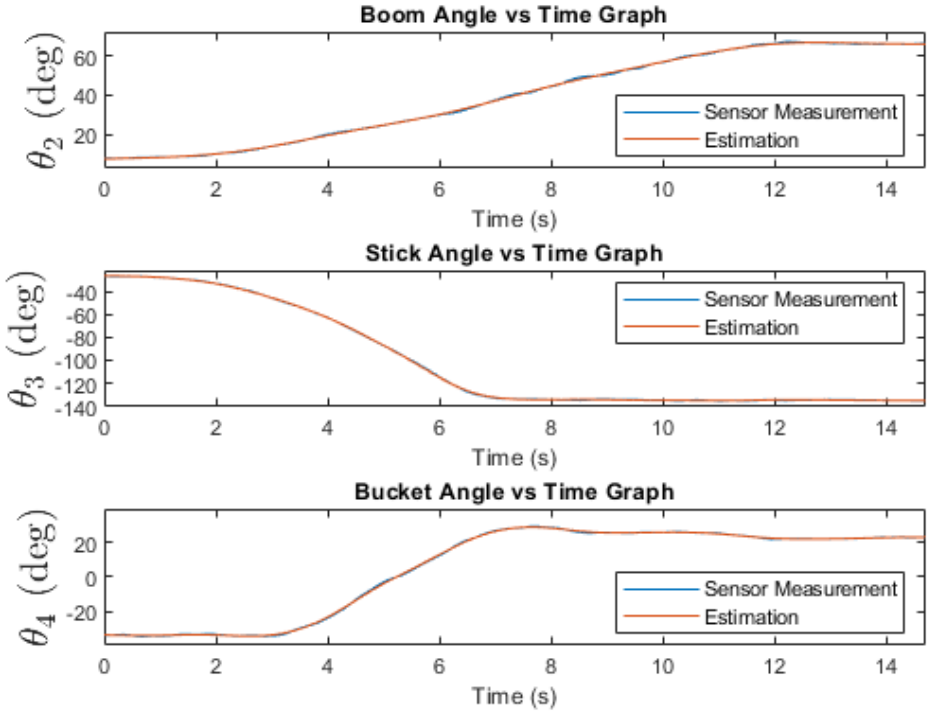

Figure A.9 *Angular position measurements and estimations, data set 4, 318 kg load*

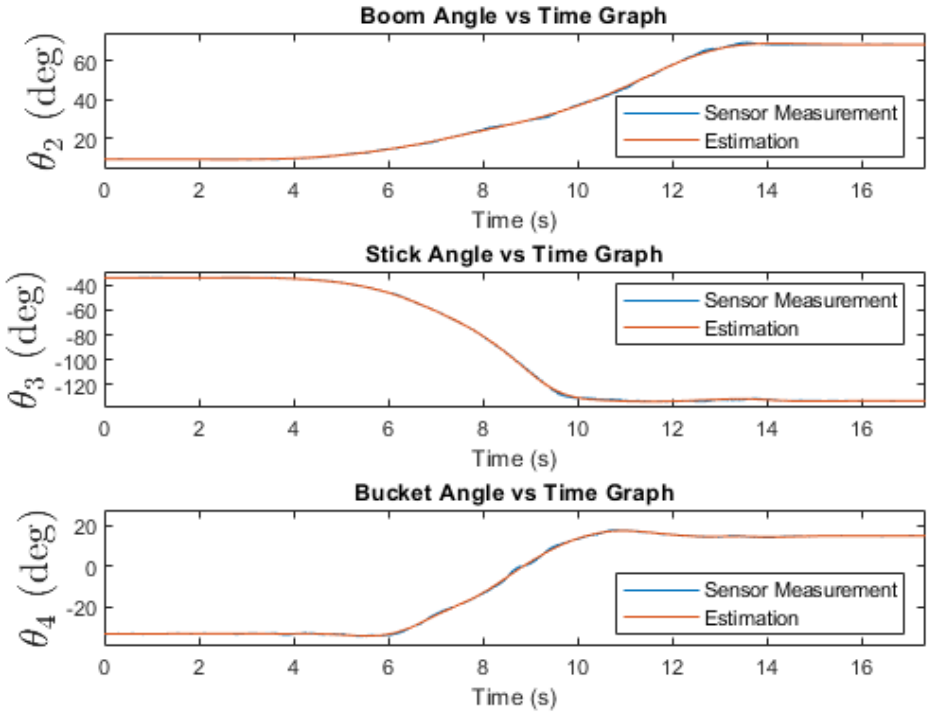

Figure A.10 *Angular position measurements and estimations, data set 5, 318 kg load*

A.3 Angular position graphs for data sets with 618 kg reference load

This section shows the angular position graphs for the data sets with 618 kg reference load in the bucket. The following Figures A.11, A.12, A.13, A.14, and A.15 represent the boom, the stick, and the bucket angular position measurements together with the fitted polynomials using smoothing splines as explained in Section 5.2.

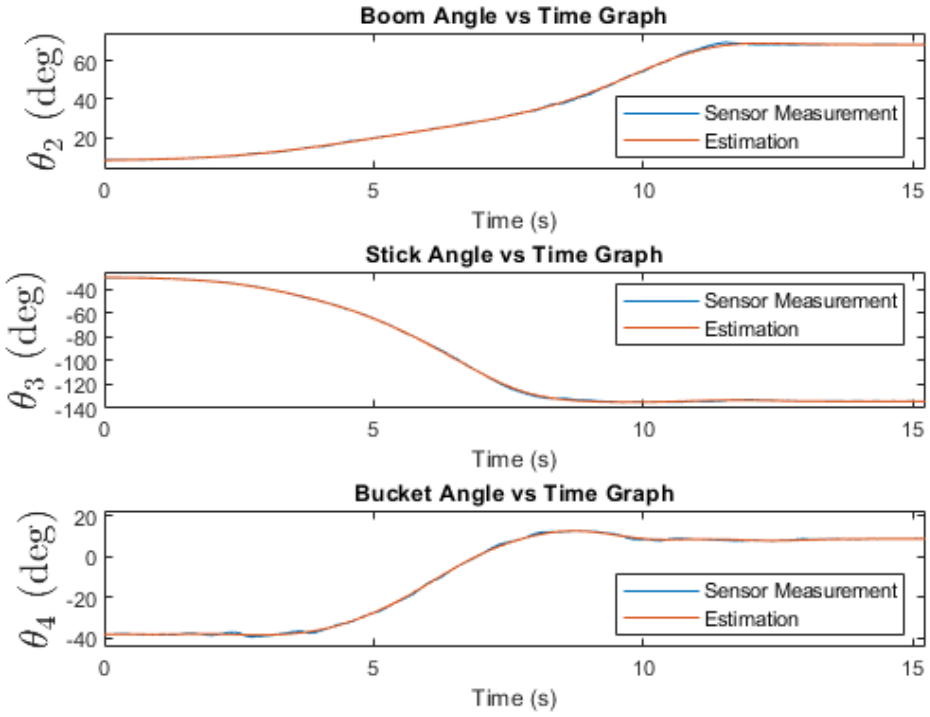

Figure A.11 *Angular position measurements and estimations, data set 1, 618 kg load*

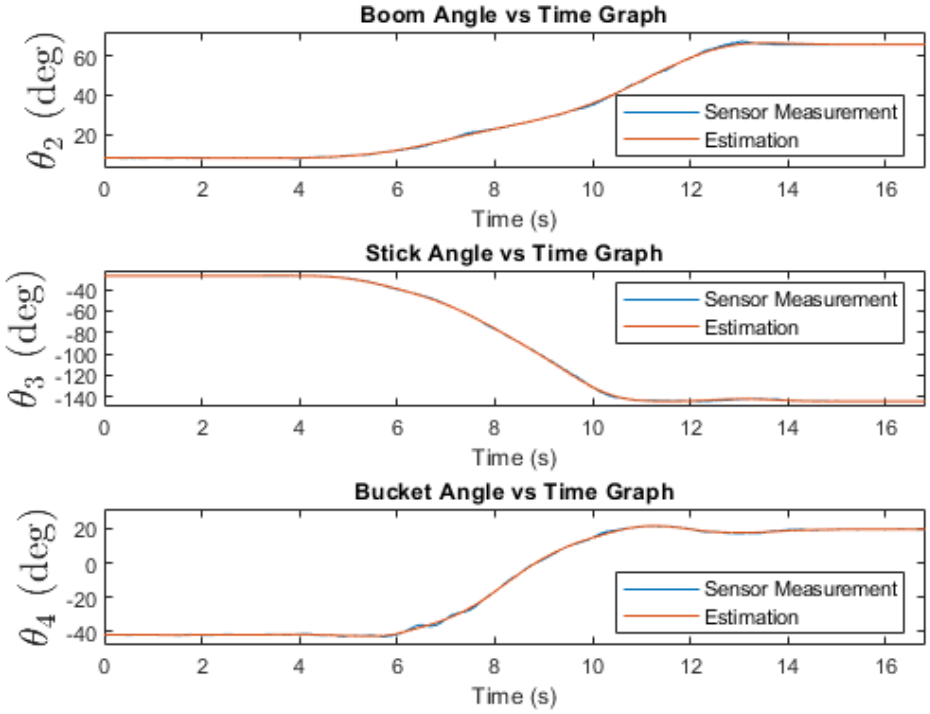

Figure A.12 *Angular position measurements and estimations, data set 2, 618 kg load*

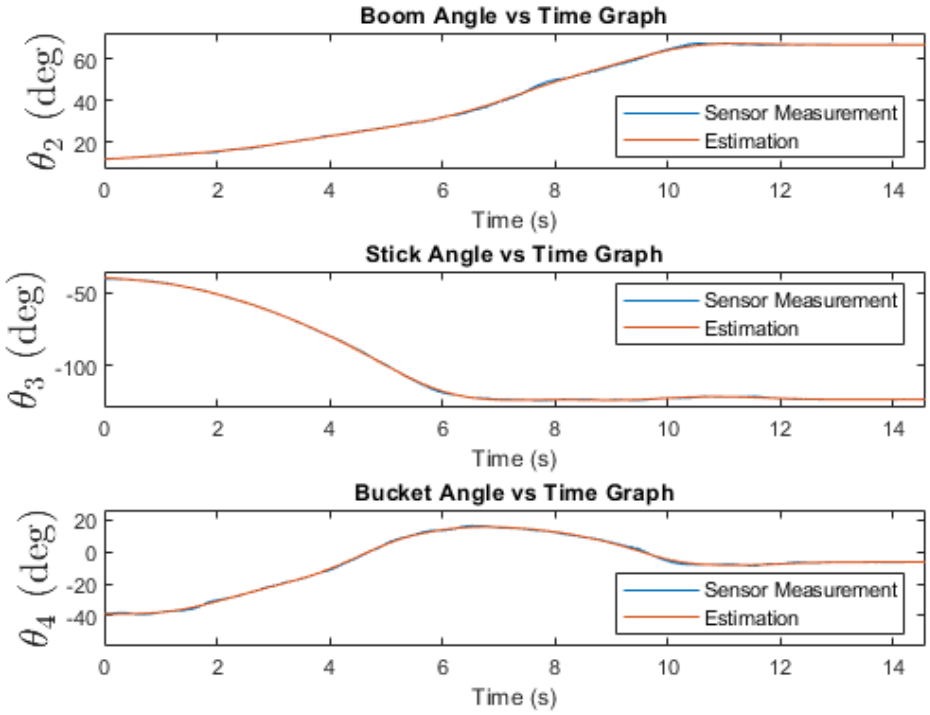

Figure A.13 *Angular position measurements and estimations, data set 3, 618 kg load*

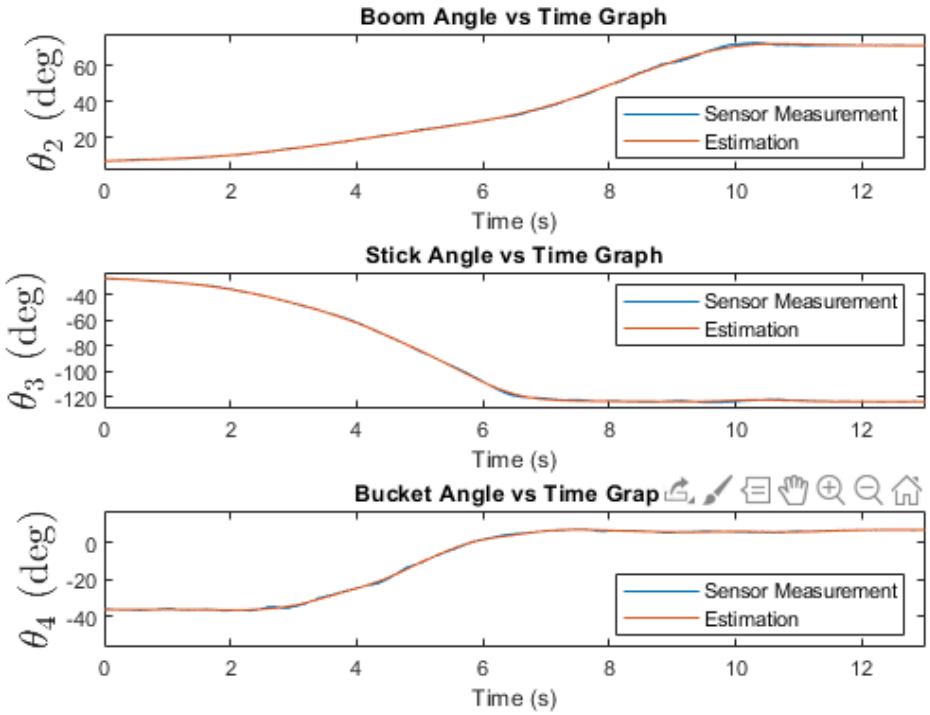

Figure A.14 *Angular position measurements and estimations, data set 4, 618 kg load*

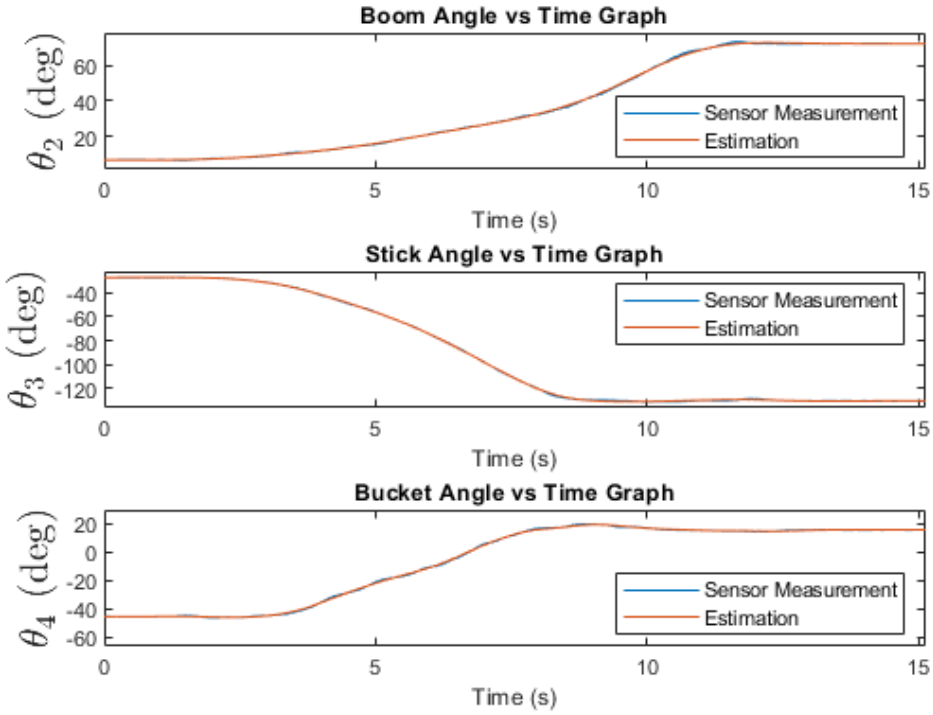

Figure A.15 *Angular position measurements and estimations, data set 5, 618 kg load*

B VISUALIZATION OF ANGULAR VELOCITY MEASUREMENTS IN DYNAMIC LOAD WEIGHT ESTIMATION

The angular velocity measurements and estimations from the boom, the stick, and the bucket links are shown in this appendix for all the data sets collected for dynamic load weight estimation. The tolerance values used in the function *spaps* are the same with the ones used in angular position estimations.

B.1 Angular velocity graphs for data sets with empty bucket

This section provides the angular velocity graphs for the data sets with empty bucket. The following Figures B.1, B.2, B.3, B.4, B.5 represent the boom, the stick, and the bucket angular position measurements together with the angular velocity estimations that are obtained by using the first derivative of the fitted polynomials on the angular position data.

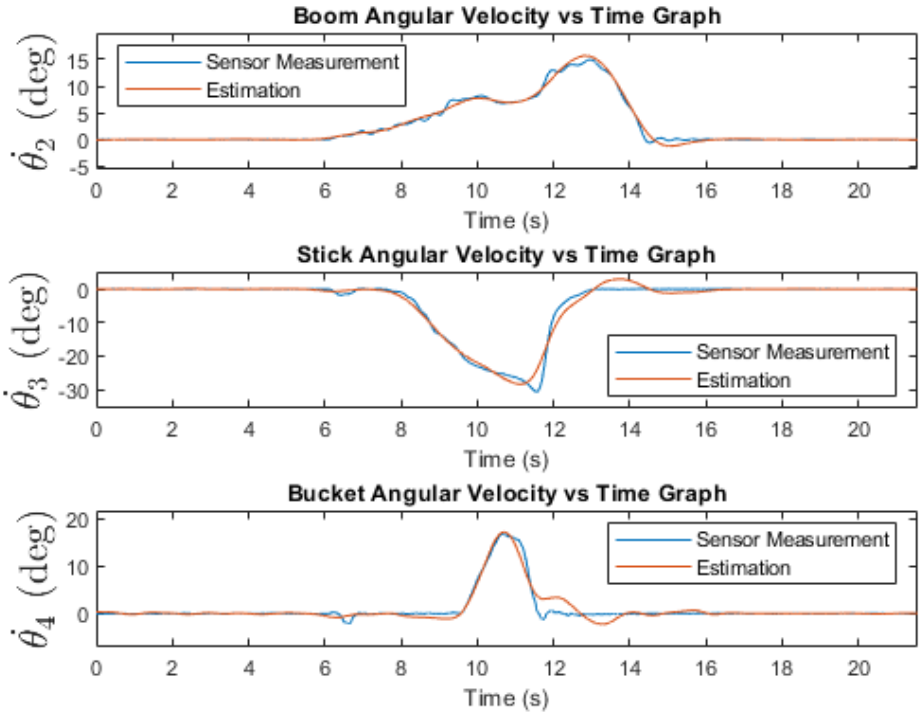

Figure B.1 *Angular velocity measurements and estimations, data set 1, empty bucket*

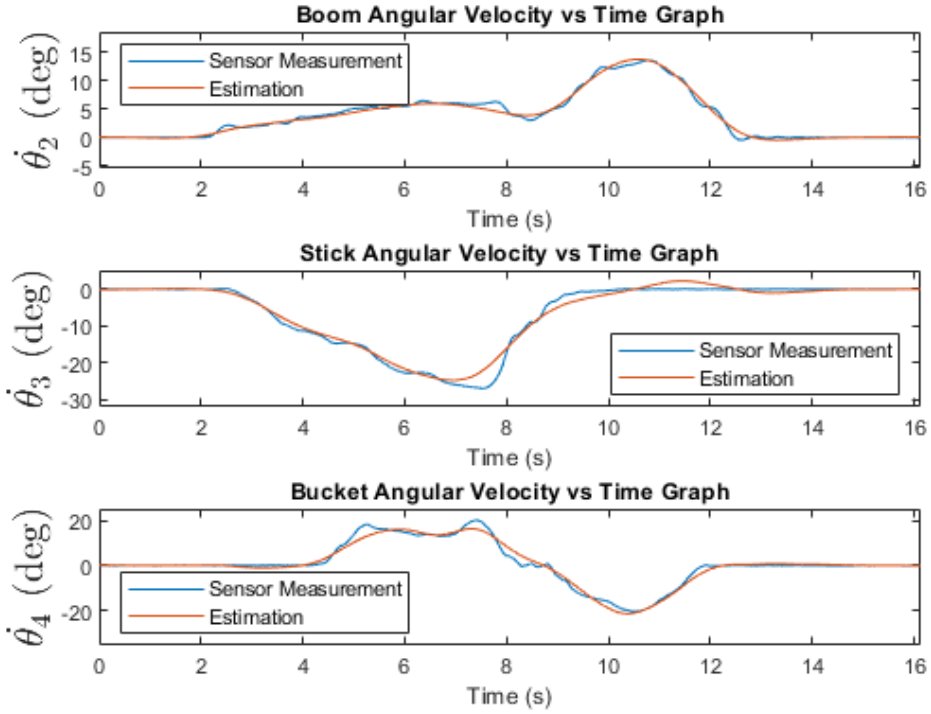

Figure B.2 *Angular velocity measurements and estimations, data set 2, empty bucket*

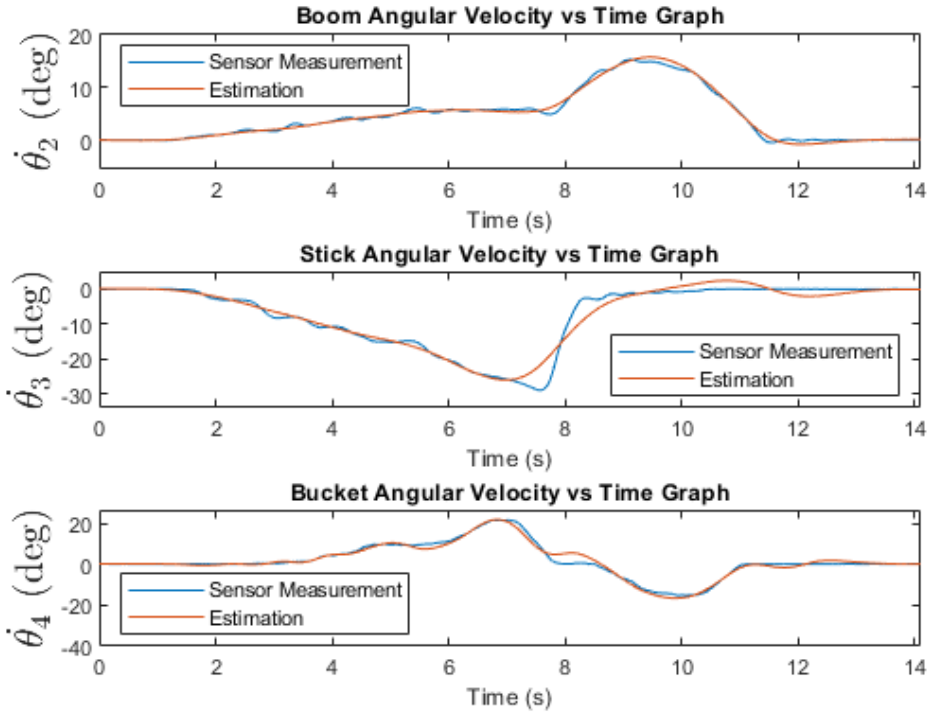

Figure B.3 *Angular velocity measurements and estimations, data set 3, empty bucket*

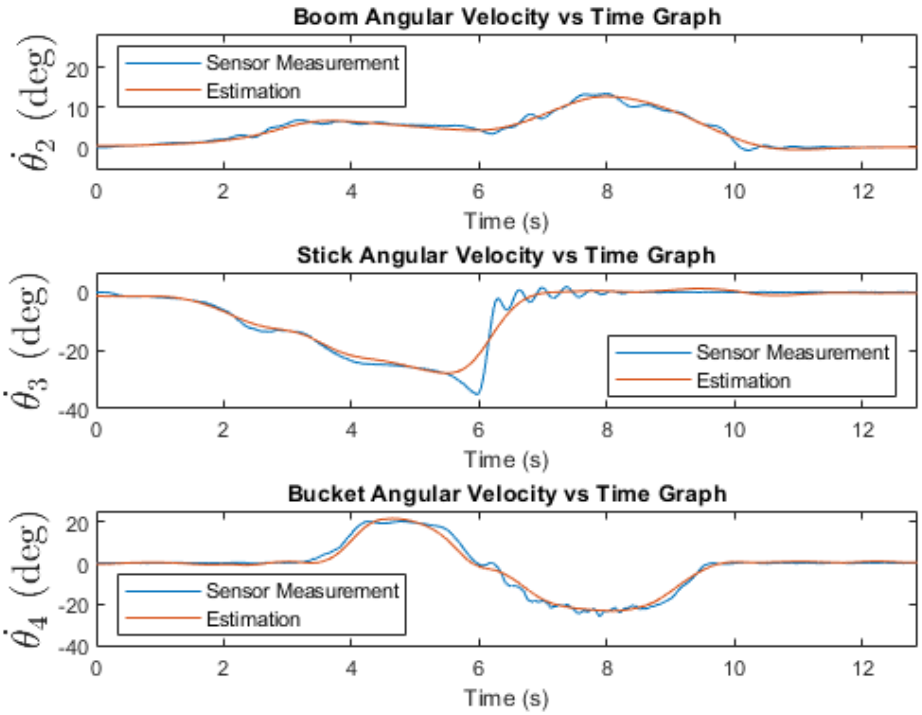

Figure B.4 *Angular velocity measurements and estimations, data set 4, empty bucket*

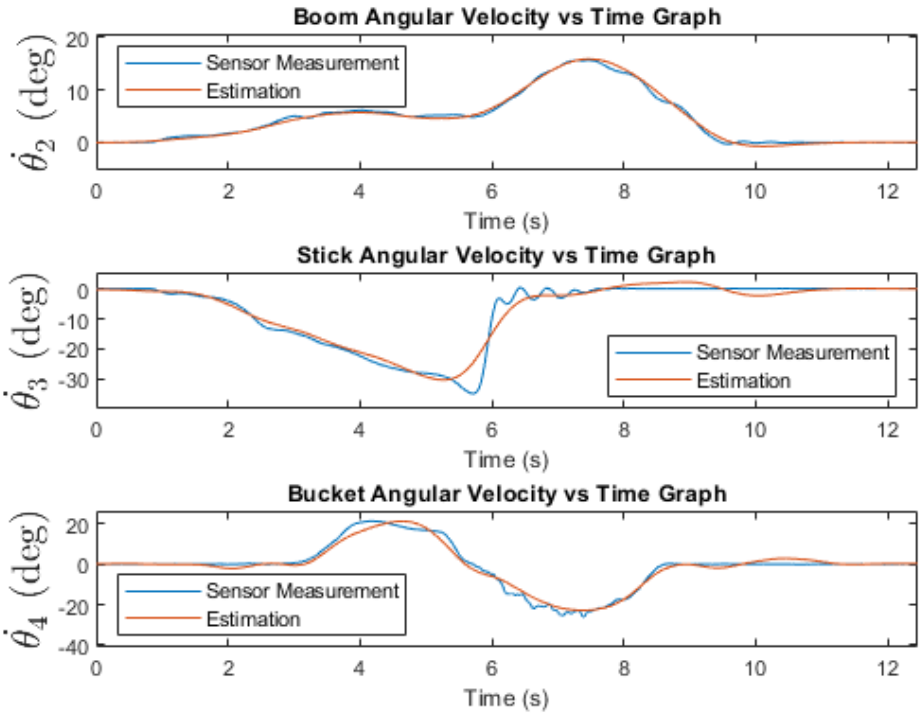

Figure B.5 *Angular velocity measurements and estimations, data set 5, empty bucket*

B.2 Angular velocity graphs for data sets with 318 kg reference load

This section provides the angular velocity graphs for the data sets with 318 kg load. The following Figures B.6, B.7, B.8, B.9, B.10 represent the boom, the stick, and the bucket angular position measurements together with the angular velocity estimations that are obtained by making use of the fitted polynomials on the angular position data.

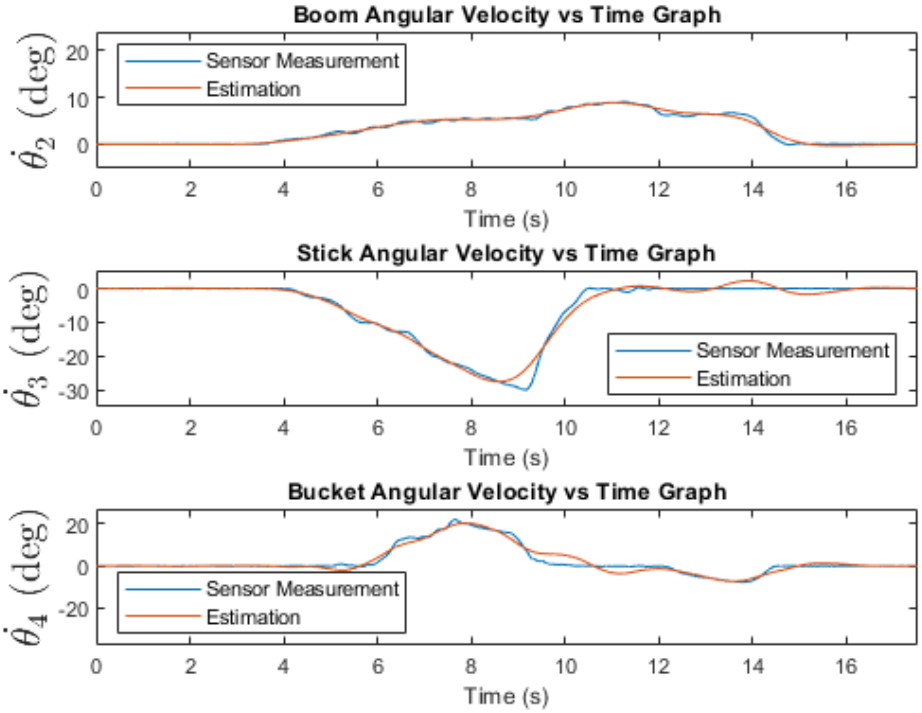

Figure B.6 *Angular velocity measurements and estimations, data set 1, 318 kg load*

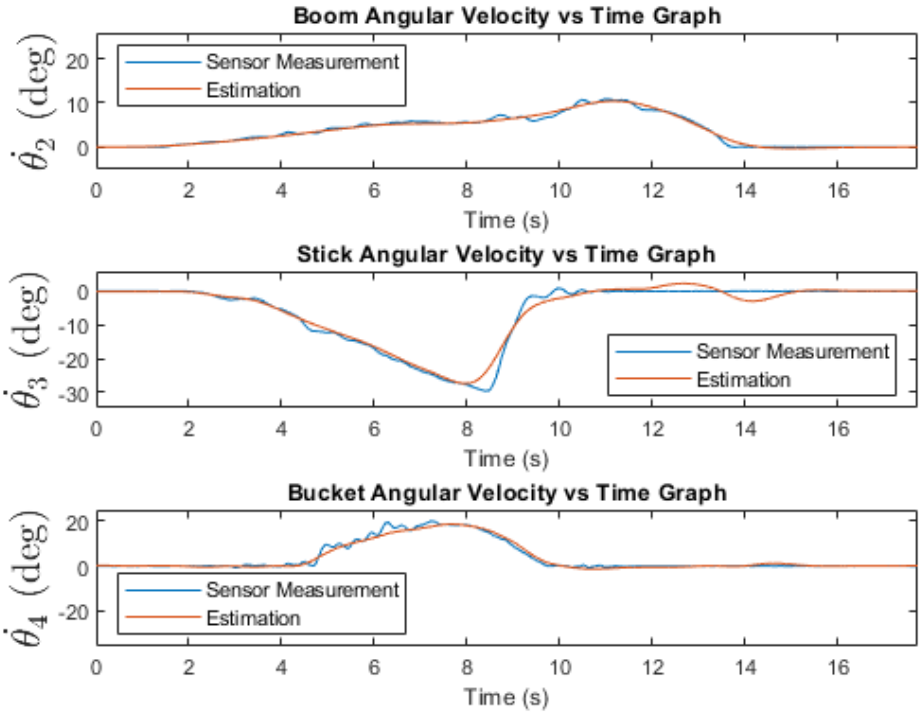

Figure B.7 *Angular velocity measurements and estimations, data set 2, 318 kg load*

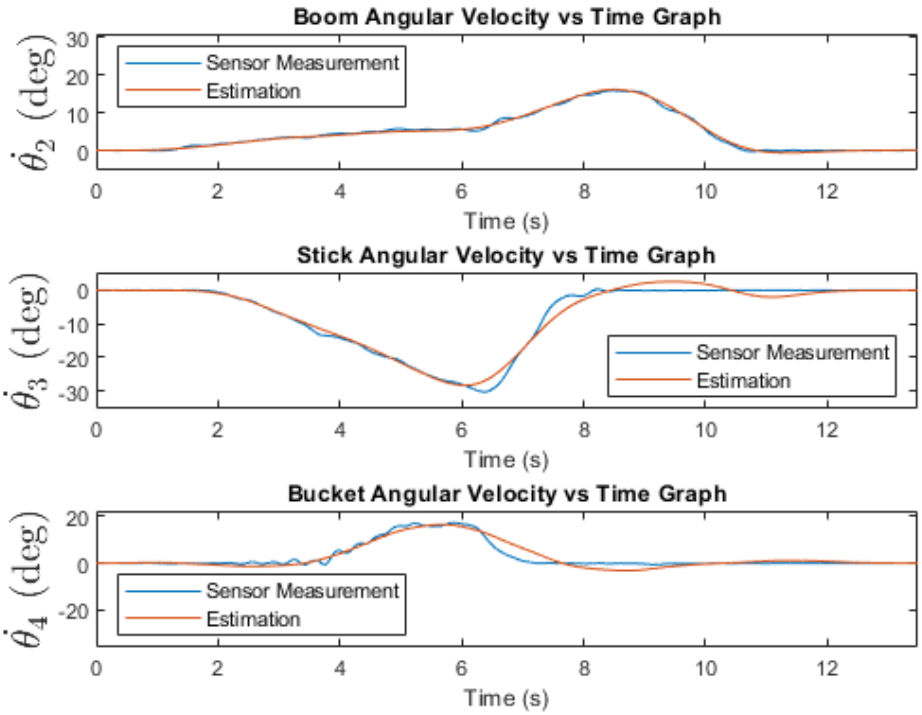

Figure B.8 *Angular velocity measurements and estimations, data set 3, 318 kg load*

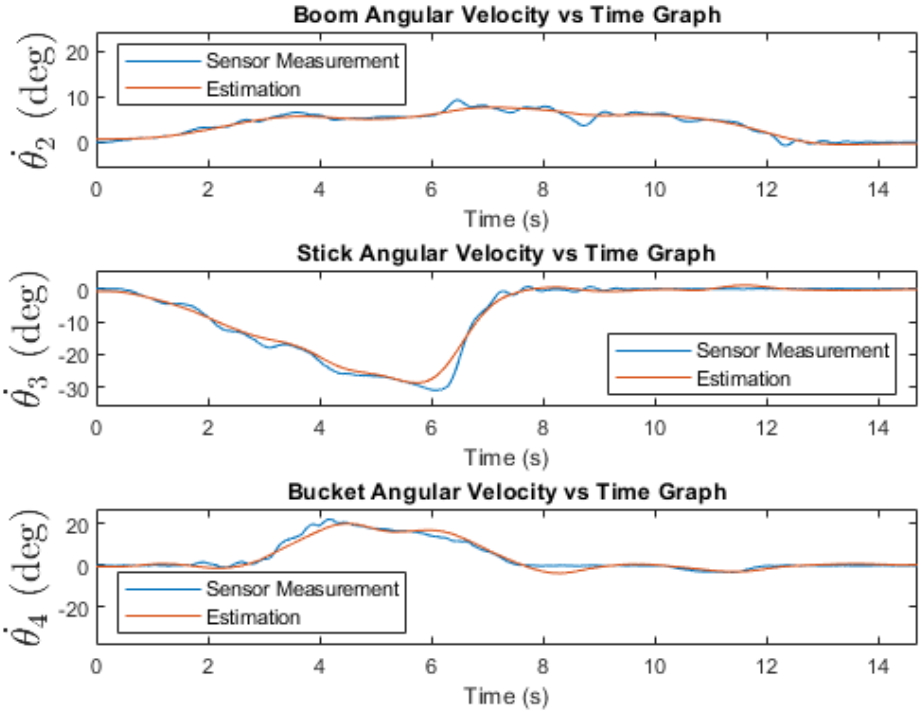

Figure B.9 *Angular velocity measurements and estimations, data set 4, 318 kg load*

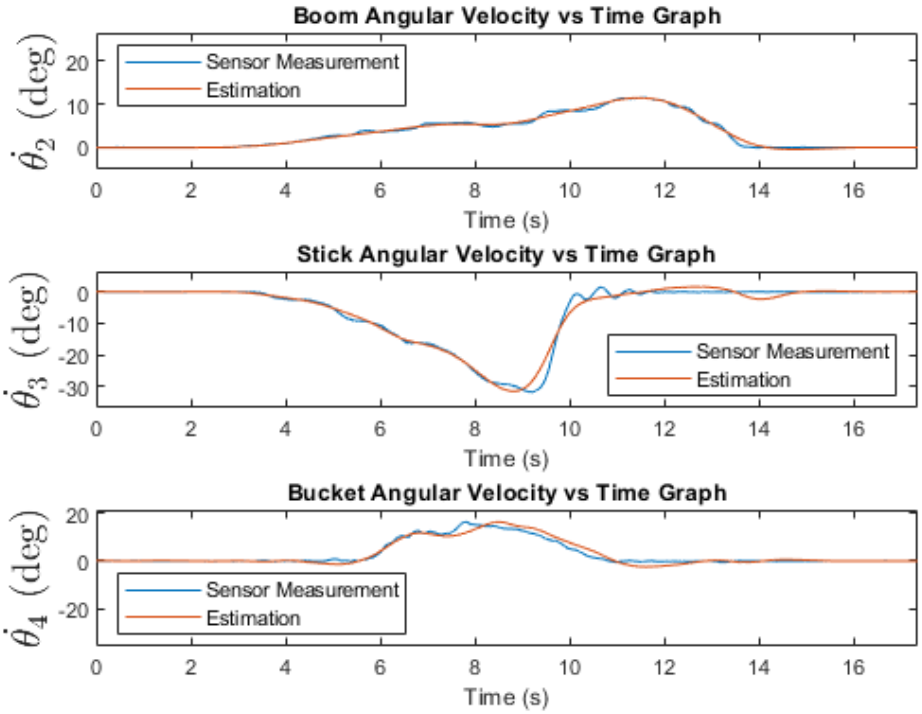

Figure B.10 *Angular velocity measurements and estimations, data set 5, 318 kg load*

B.3 Angular velocity graphs for data sets with 618 kg reference load

This section provides the angular velocity graphs for the data sets with 618 kg load. The following Figures B.11, B.12, B.13, B.14, B.15 represent the boom, the stick, and the bucket angular position measurements together with the angular velocity estimations that are obtained by using the first derivative of the fitted polynomials on the angular position data.

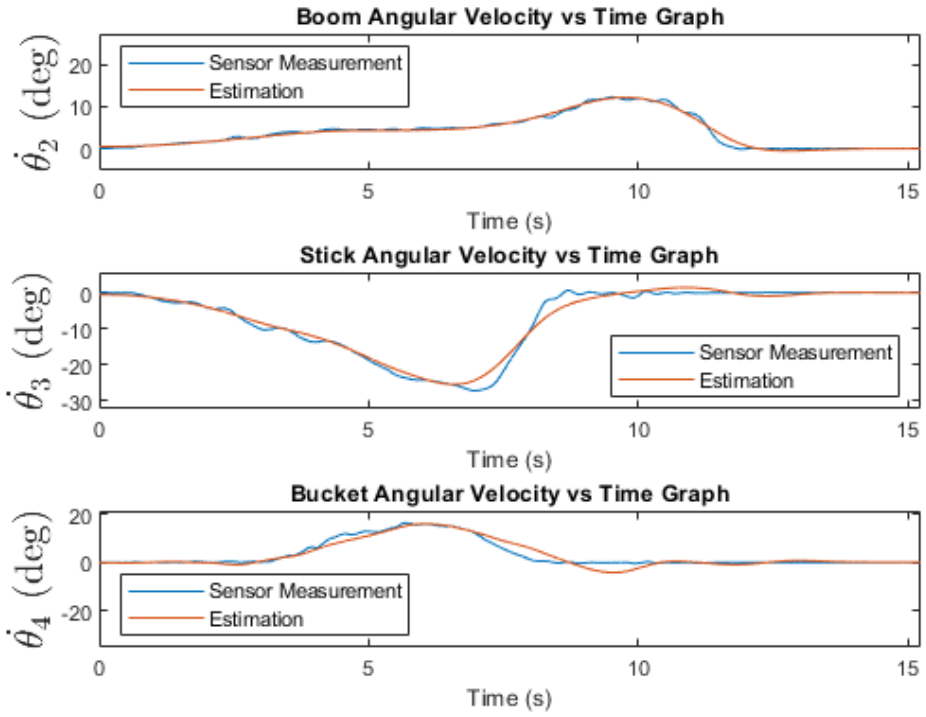

Figure B.11 *Angular velocity measurements and estimations, data set 1, 618 kg load*

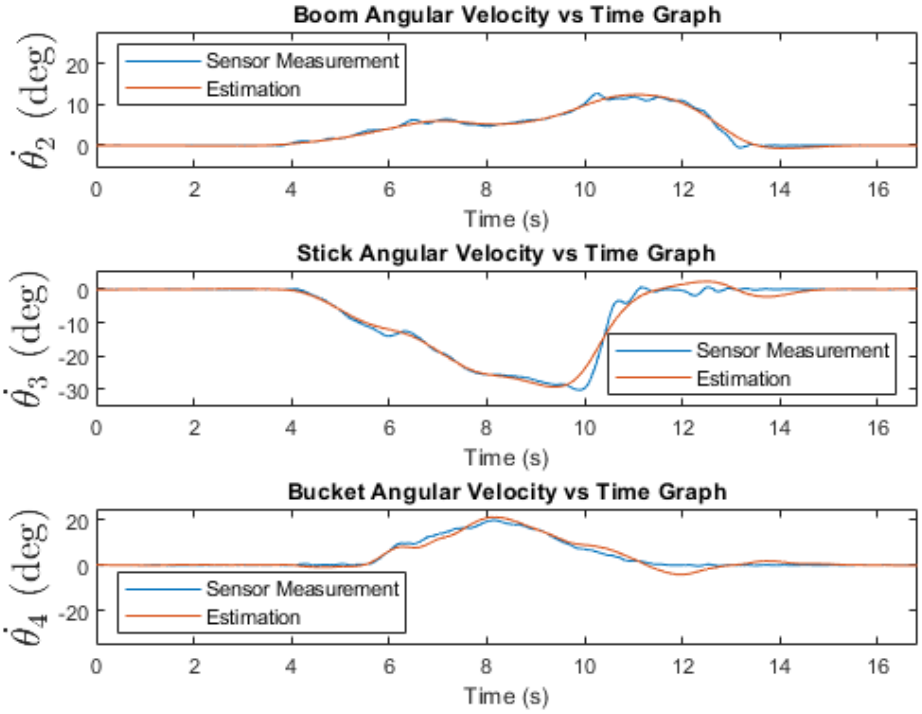

Figure B.12 *Angular velocity measurements and estimations, data set 2, 618 kg load*

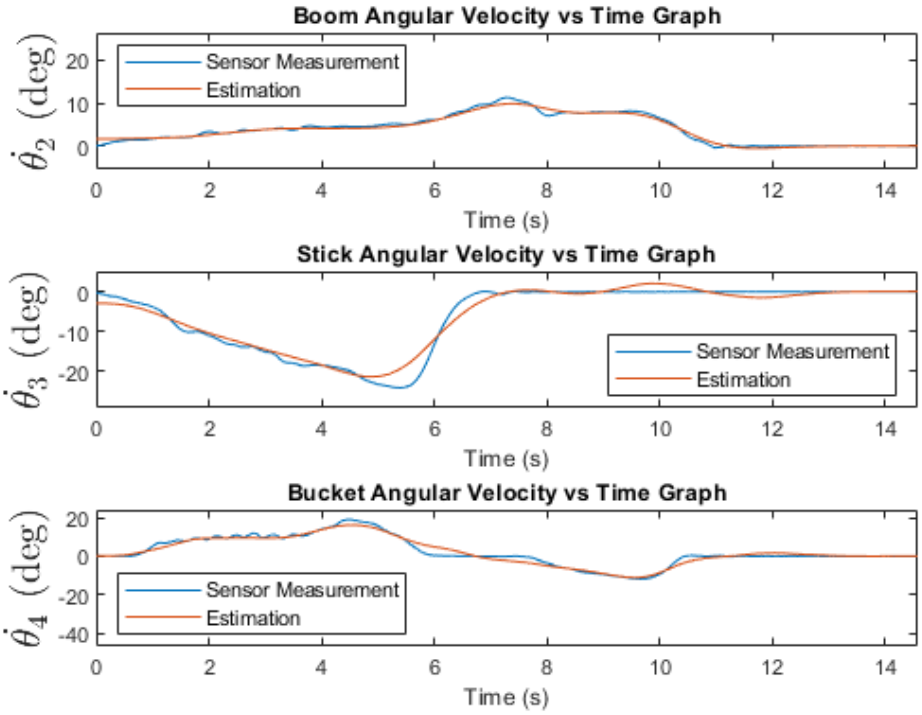

Figure B.13 *Angular velocity measurements and estimations, data set 3, 618 kg load*

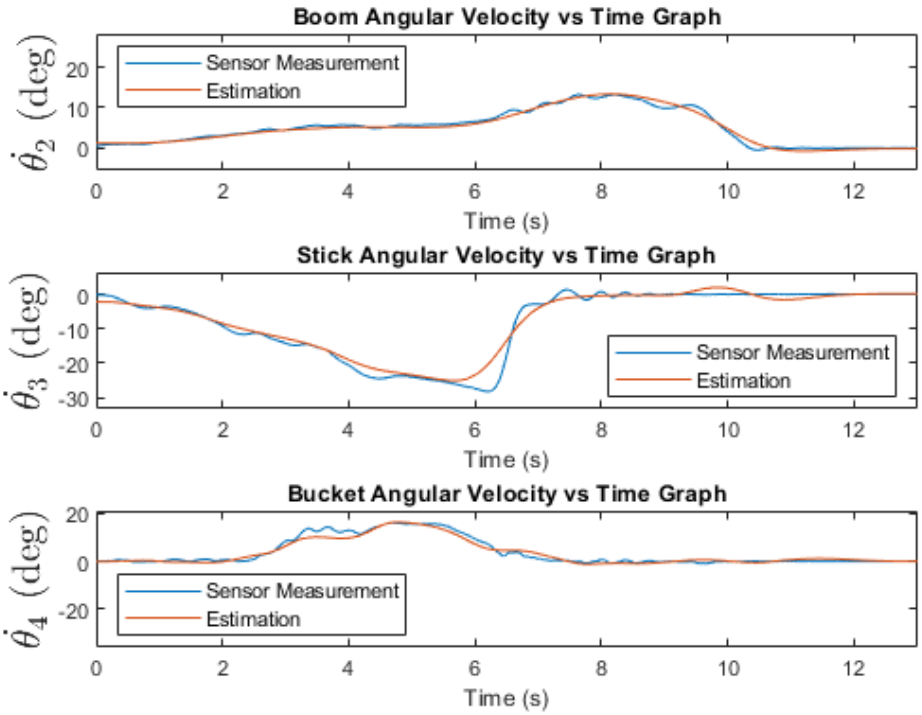

Figure B.14 *Angular velocity measurements and estimations, data set 4, 618 kg load*

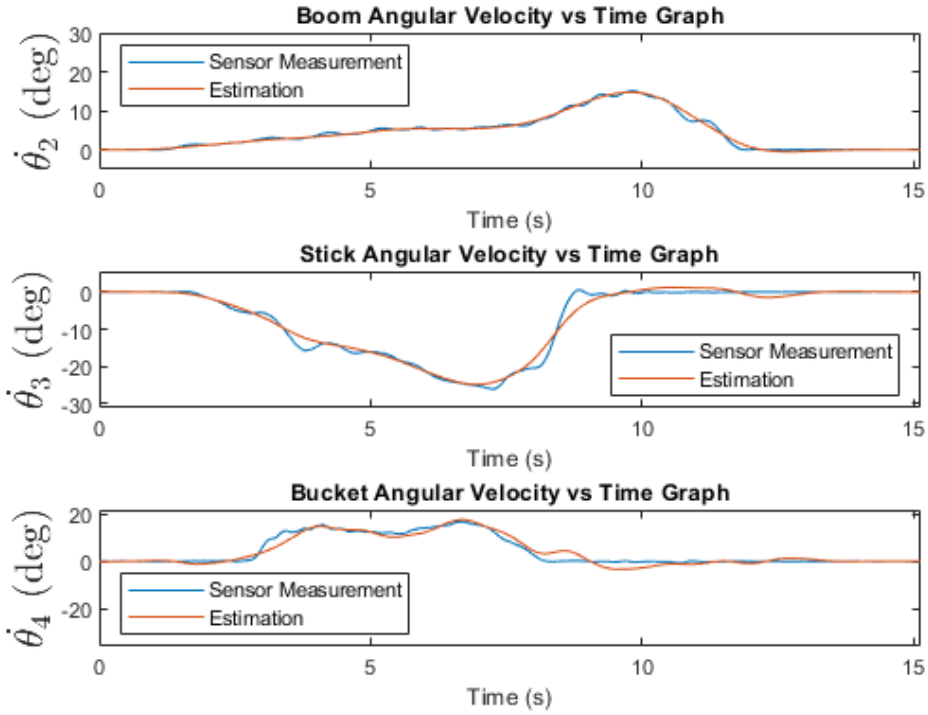

Figure B.15 *Angular velocity measurements and estimations, data set 5, 618 kg load*

C VISUALIZATION OF ANGULAR ACCELERATION ESTIMATIONS FOR DYNAMIC LOAD WEIGHT ESTIMATION

The angular acceleration estimations for the boom, the stick, and the bucket links are plotted in this appendix for all the data sets collected for dynamic load weight estimation.

C.1 Angular acceleration graphs for data sets with empty bucket

This section provides the angular acceleration graphs for the data sets with empty bucket. The following Figures C.1, C.2, C.3, C.4, C.5 illustrate the estimated angular acceleration values.

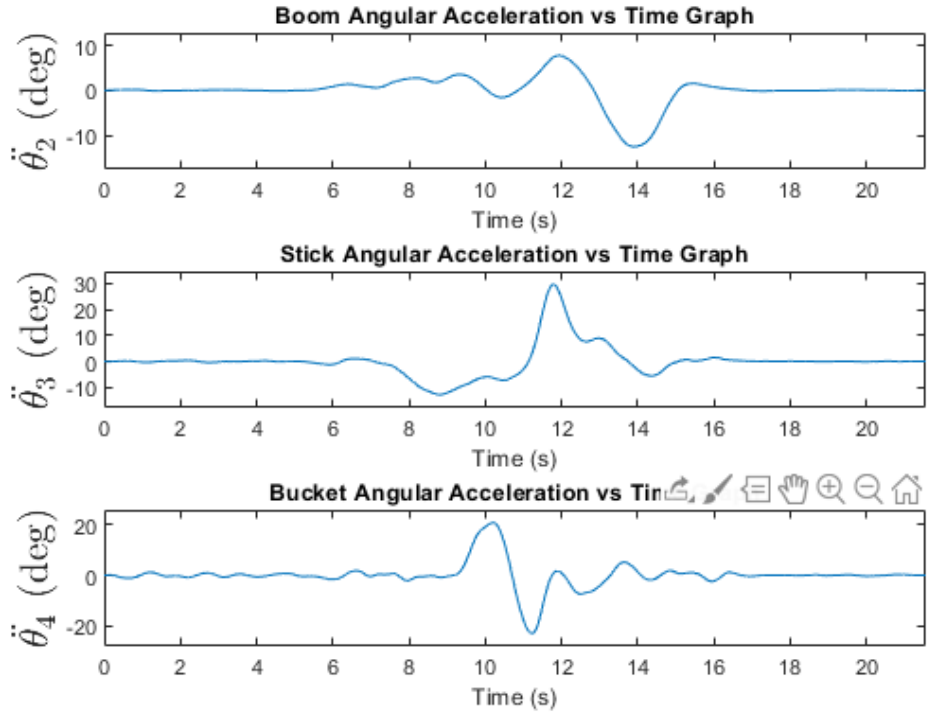

Figure C.1 *Angular acceleration estimations, data set 1, empty bucket*

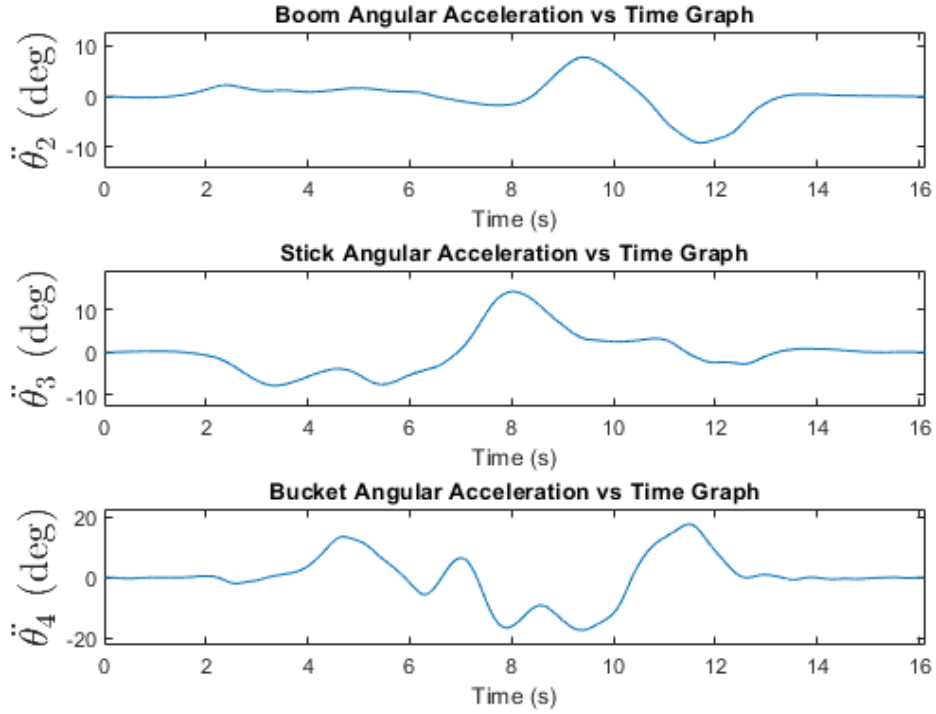

Figure C.2 *Angular acceleration estimations, data set 2, empty bucket*

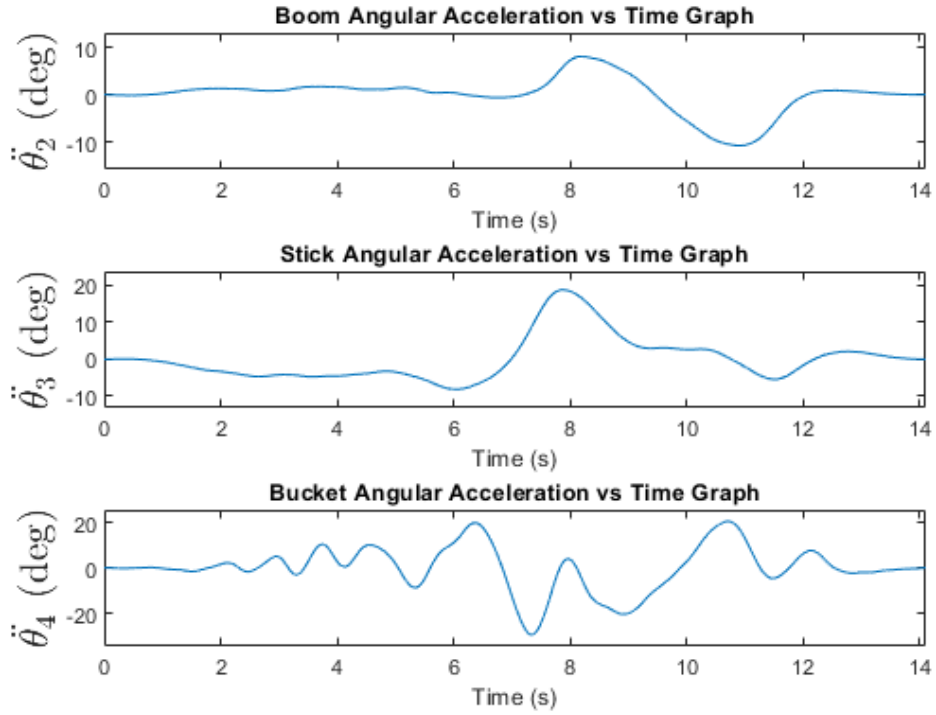

Figure C.3 *Angular acceleration estimations, data set 3, empty bucket*

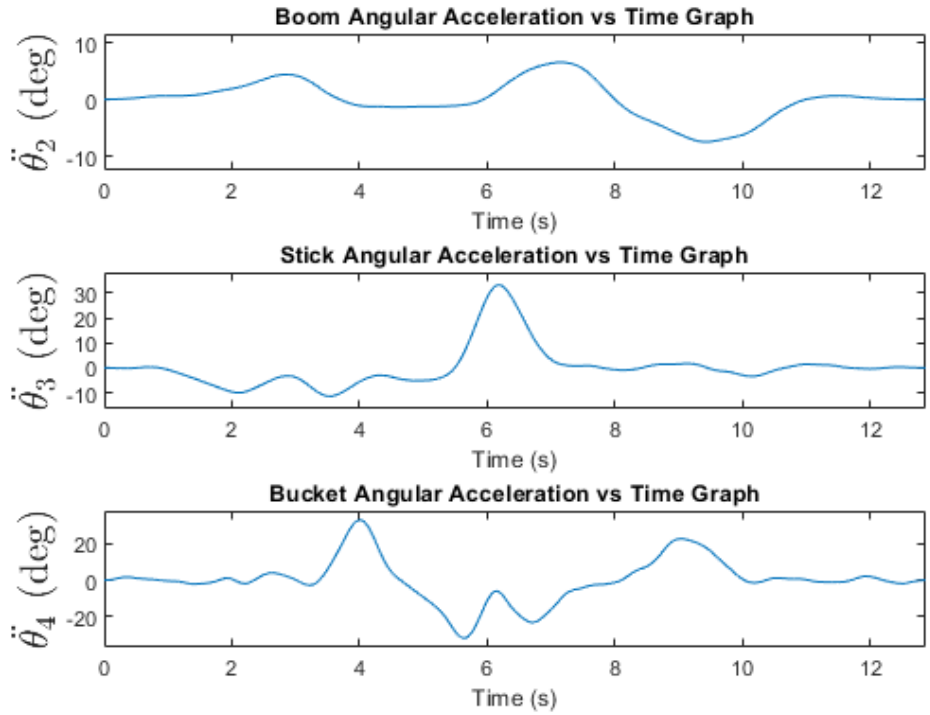

Figure C.4 *Angular acceleration estimations, data set 4, empty bucket*

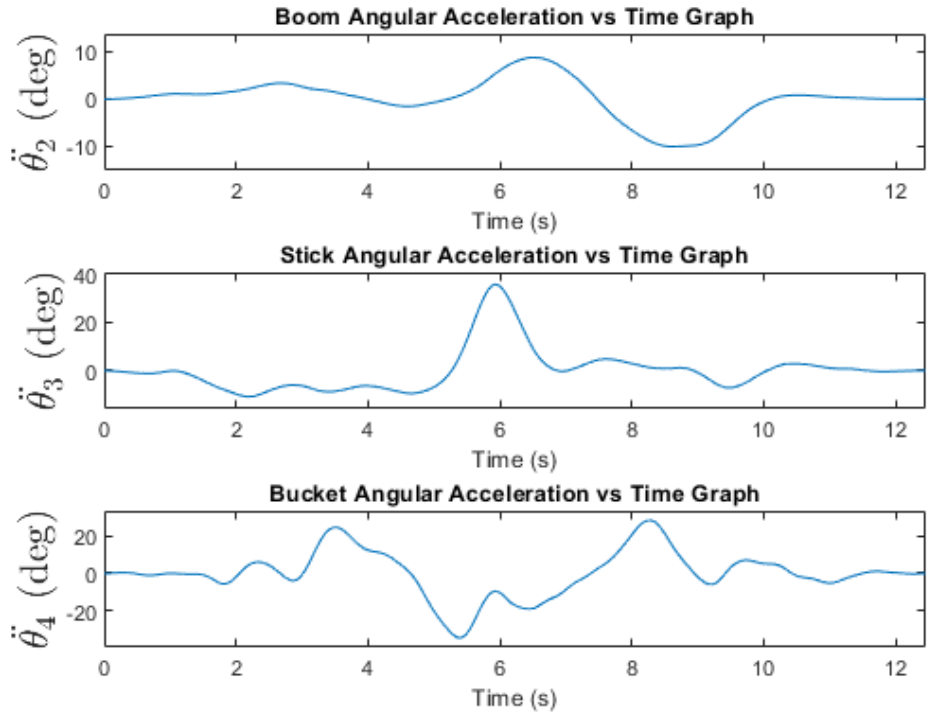

Figure C.5 *Angular acceleration estimations, data set 5, empty bucket*

C.2 Angular acceleration graphs for data sets with 318 kg reference load

This section provides the angular acceleration graphs for the data sets with 318 kg load. The following Figures C.6, C.7, C.8, C.9, C.10 illustrate the estimated angular acceleration values.

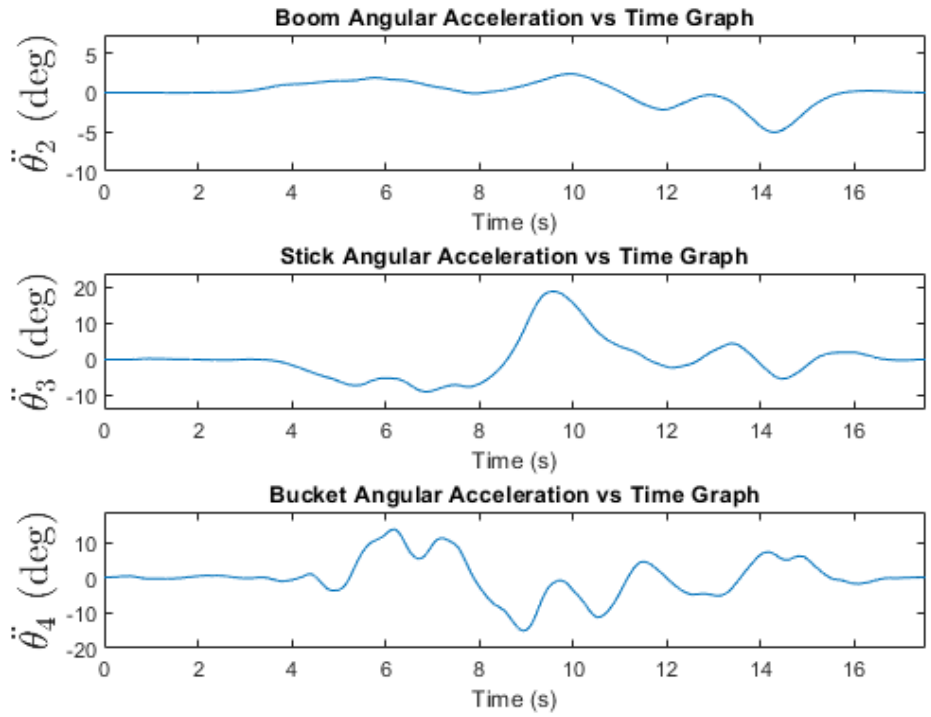

Figure C.6 *Angular acceleration estimations, data set 1, 318 kg load*

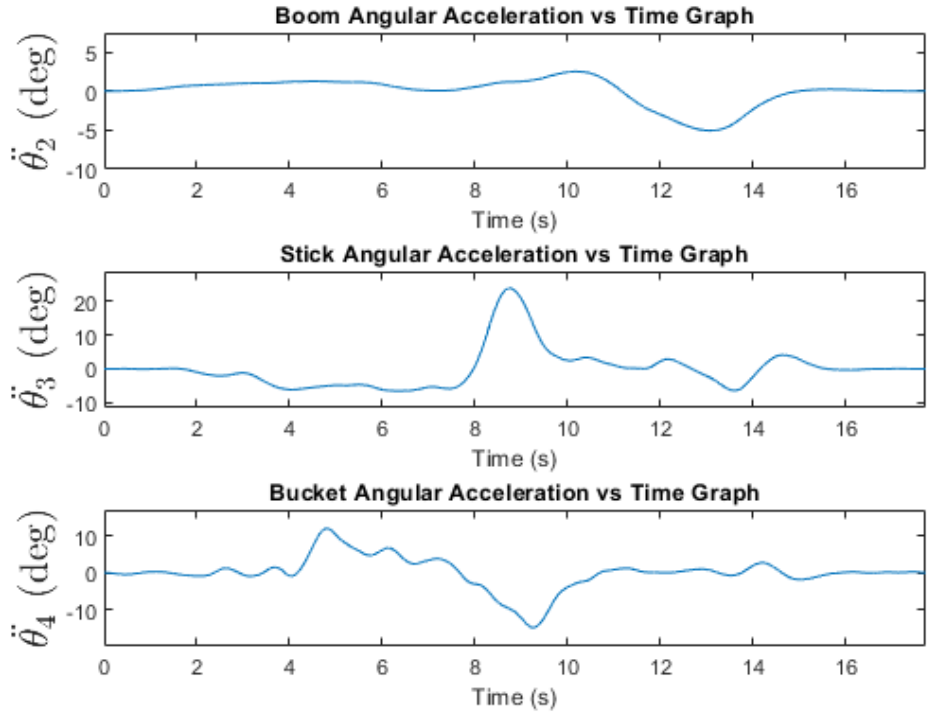

Figure C.7 *Angular acceleration estimations, data set 2, 318 kg load*

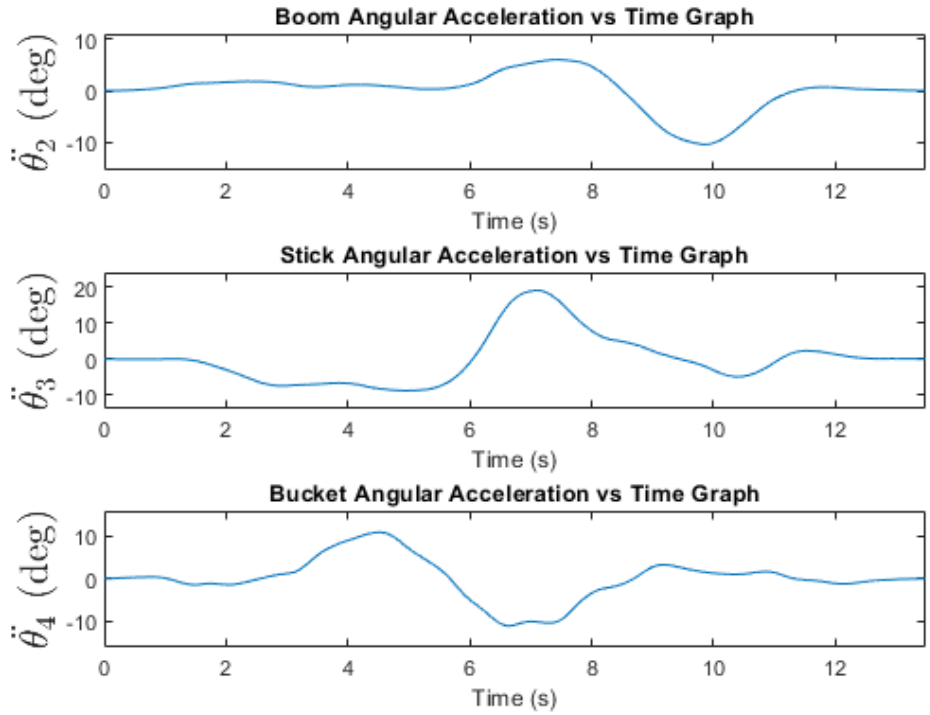

Figure C.8 *Angular acceleration estimations, data set 3, 318 kg load*

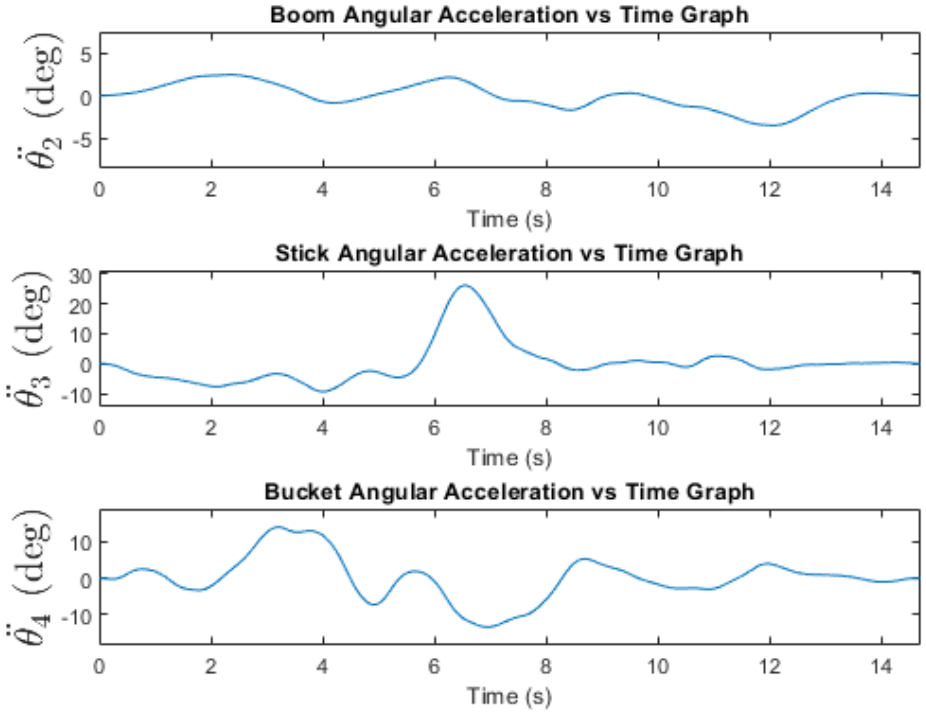

Figure C.9 *Angular acceleration estimations, data set 4, 318 kg load*

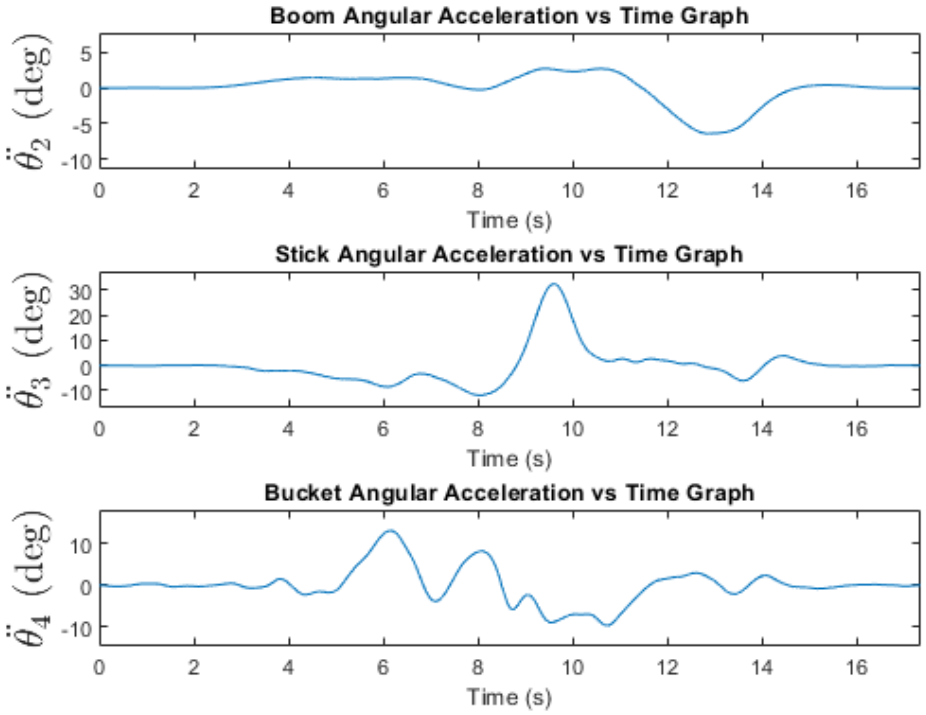

Figure C.10 *Angular acceleration estimations, data set 5, 318 kg load*

C.3 Angular acceleration graphs for data sets with 618 kg reference load

This section provides the angular acceleration graphs for the data sets with 618 kg load. The following Figures C.11, C.12, C.13, C.14, C.15 visualize the estimated angular acceleration values.

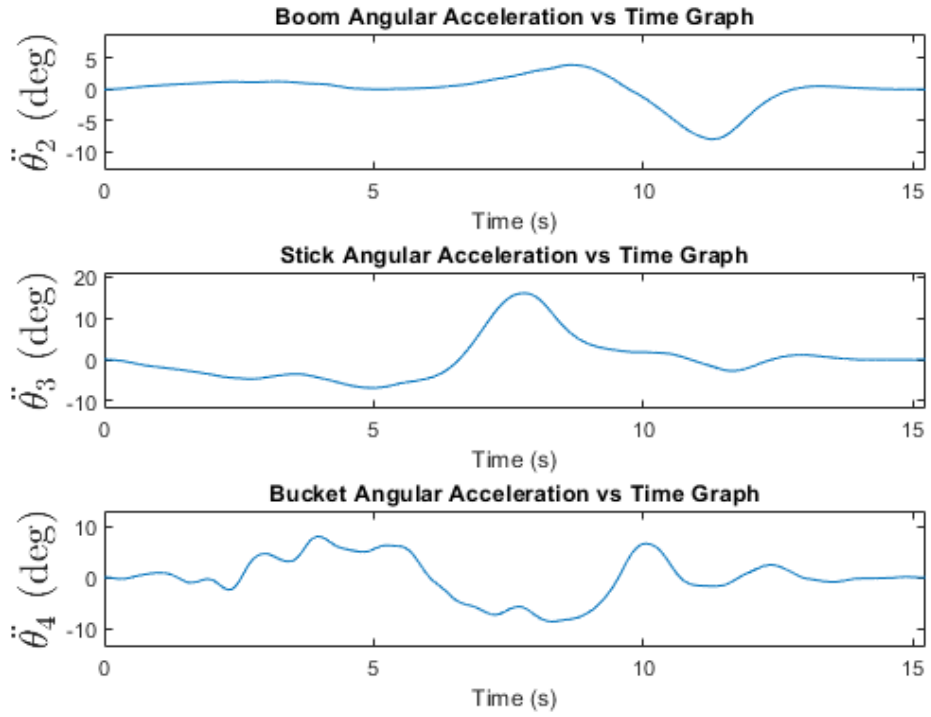

Figure C.11 *Angular acceleration estimations, data set 1, 618 kg load*

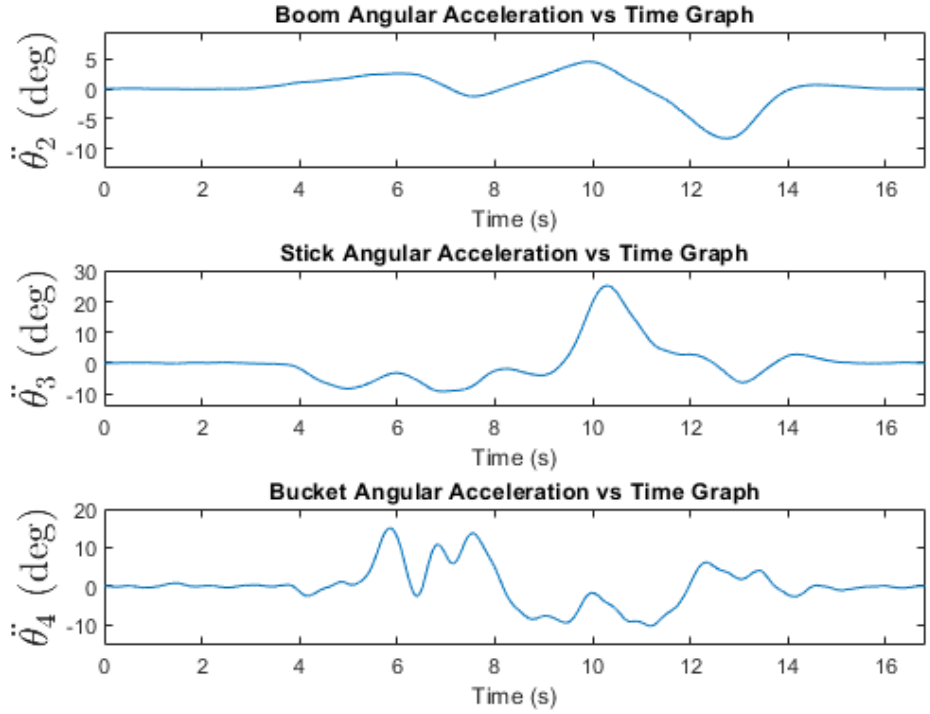

Figure C.12 *Angular acceleration estimations, data set 2, 618 kg load*

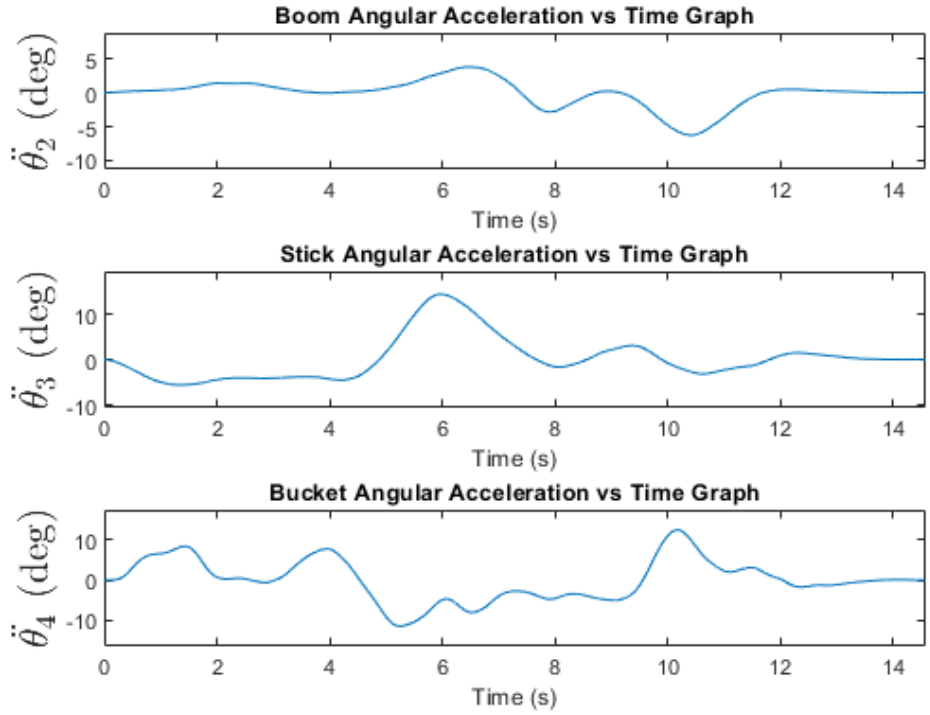

Figure C.13 *Angular acceleration estimations, data set 3, 618 kg load*

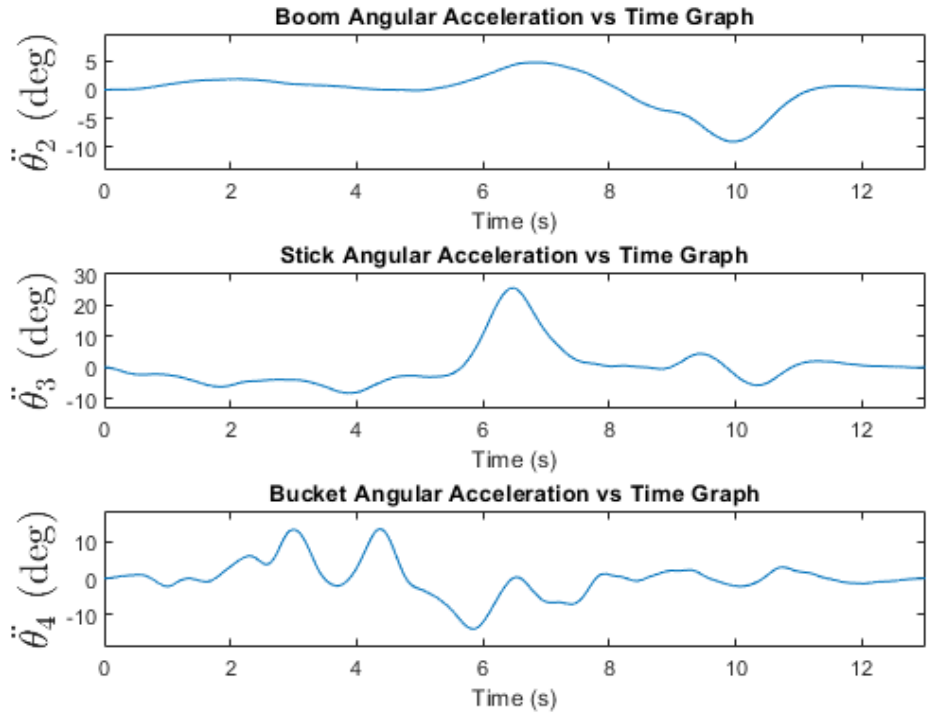

Figure C.14 *Angular acceleration estimations, data set 4, 618 kg load*

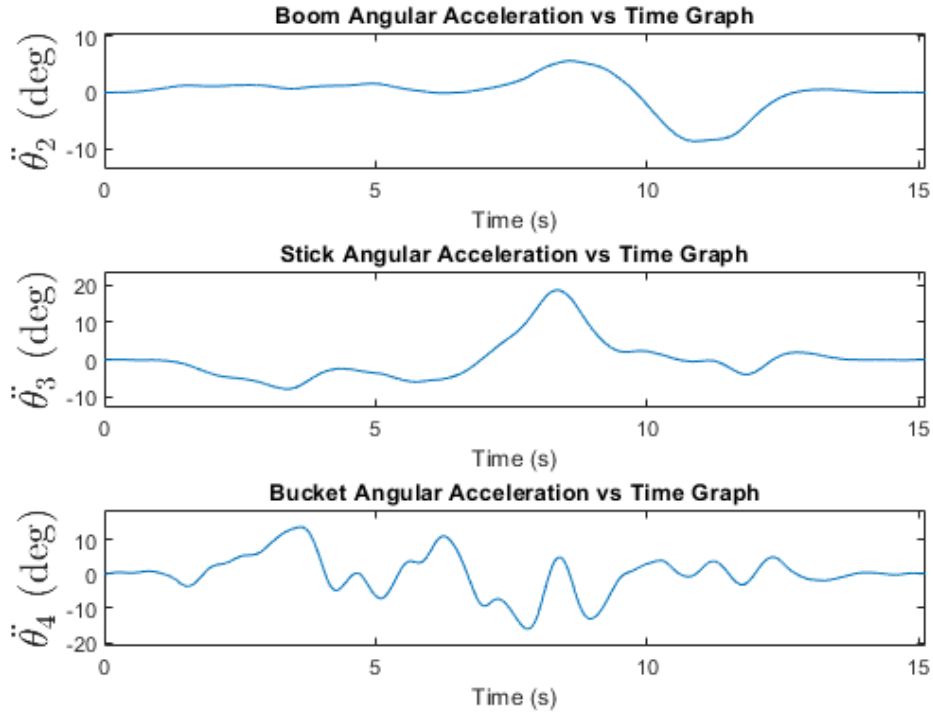

Figure C.15 *Angular acceleration estimations, data set 5, 618 kg load*